Science of the Total Environment 860 (2023) 160480

Contents lists available at ScienceDirect

Science of the Total Environment

journal homepage: www.elsevier.com/locate/scitotenv

Fracking wastewater treatment: Catalytic performance and life cycle environmental impacts of cerium-based mixed oxide catalysts for catalytic wet oxidation of organic compounds

Xiaoxia Ou [a,b,*,1], Marco Tomatis [a,1], Billy Payne [a], Helen Daly [a], Sarayute Chansai [a], Xiaolei Fan [a], Carmine D'Agostino [a,c], Adisa Azapagic [a,**], Christopher Hardacre [a,**]

[a] Department of Chemical Engineering, School of Engineering, The University of Manchester, Oxford Road, Manchester M13 9PL, UK
[b] Nottingham Ningbo China Beacons of Excellence Research and Innovation Institute, 211 Xingguang Road, Ningbo, China
[c] Dipartimento di Ingegneria Civile, Chimica, Ambientale e dei Materiali (DICAM), Alma Mater Studiorum – Università di Bologna, Via Terracini, 28, 40131 Bologna, Italy

HIGHLIGHTS

- Catalytic wet oxidation with $MnCeO_x$ removes 94 % of organics.
- $CuCeO_x$ is much less efficient and leads to severe copper leaching.
- $MnCeO_x$ has 12–98 % lower life cycle environmental impacts than $CuCeO_x$.
- The impacts of catalytic wet oxidation are 94–99 % lower than of ozonation.
- Catalytic treatment improves the overall environmental sustainability of fracking.

GRAPHICAL ABSTRACT

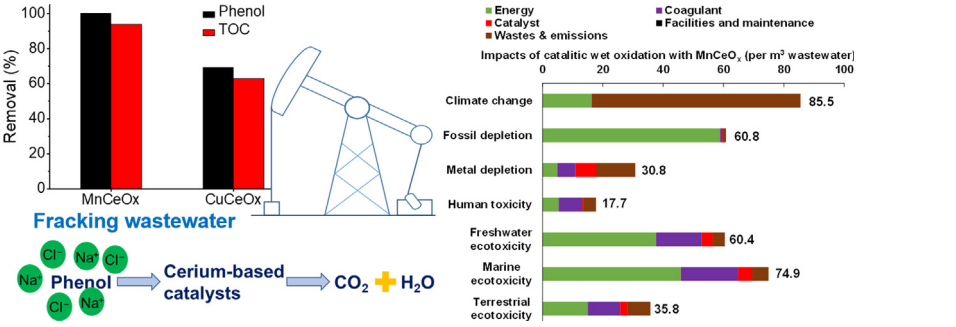

ARTICLE INFO

Editor: Deyi Hou

Keywords:
Shale gas
Wastewater treatment
Cerium-based mixed oxide
Catalytic wet oxidation
Life cycle assessment
Environmental impacts

ABSTRACT

Water scarcity and the consequent increase of freshwater prices are a cause for concern in regions where shale gas is being extracted via hydraulic fracturing. Wastewater treatment methods aimed at reuse/recycle of fracking wastewater can help reduce water stress of the fracking process. Accordingly, this study assessed the catalytic performance and life cycle environmental impacts of cerium-based mixed oxide catalysts for catalytic wet oxidation (CWO) of organic contaminants, in order to investigate their potential as catalysts for fracking wastewater treatment. For these purposes, $MnCeO_x$ and $CuCeO_x$ were tested for phenol removal in the presence of concentrated NaCl (200 g L^{-1}), which represented a synthetic fracking wastewater. Removal of phenol in pure ("phenolic") water without NaCl was also considered for comparison. Complete (100 %) phenol and a 94 % total organic carbon (TOC) removal were achieved in both the phenolic and fracking wastewaters by utilising $MnCeO_x$ (5 g L^{-1}) and insignificant metal leaching was observed. However, a much lower activity was observed when the same amount of $CuCeO_x$ was utilised: 23.3 % and 20.5 % for phenol and TOC removals, respectively, in the phenolic, and 69.1 % and 63 % in the fracking wastewater. Furthermore, severe copper leaching from $CuCeO_x$ was observed during stability tests conducted in the fracking wastewater. A life cycle assessment (LCA) study carried out as part of this work showed that the production of $MnCeO_x$ had 12–98 % lower impacts than $CuCeO_x$ due to the higher impacts of copper than manganese precursors. Furthermore, the environmental impacts of CWO were found to be 94–99 % lower than those of ozonation due to lower energy

* Correspondence to: X. Ou, Nottingham Ningbo China Beacons of Excellence Research and Innovation Institute, 211 Xingguang Road, Ningbo, China.
** Corresponding authors.
E-mail addresses: Xiaoxia.Ou@nottingham.edu.cn (X. Ou), Adisa.Azapagic@manchester.ac.uk (A. Azapagic), c.hardacre@manchester.ac.uk (C. Hardacre).
[1] Joint first authors.

http://dx.doi.org/10.1016/j.scitotenv.2022.160480
Received 27 June 2022; Received in revised form 29 October 2022; Accepted 21 November 2022
Available online 24 November 2022

and material requirements. Overall, the results of this study suggest that the adoption of catalytic treatment would improve both the efficiency and the environmental sustainability of both the fracking wastewater treatment and the fracking process as a whole.

1. Introduction

Natural gas extracted from shale formations is commonly known as shale gas. The relative abundance and low price of this unconventional source of natural gas (Li et al., 2022; Wang and Li, 2019) makes shale gas a suitable substitute for coal in the energy sector and other industrial activities, potentially reducing the carbon emissions of various industries (Bellani et al., 2021) in the transitional period before a wider deployment of renewables. Moreover, shale gas production can help to improve national energy security, depending on the extent of the reserves and the technical/economic feasibility of extraction.

Hydraulic fracturing is commonly utilised for the extraction of shale gas. However, this extraction method requires large volumes of water (10,000–22,000 m^3 per well) to force the release of entrapped hydrocarbons from the reservoirs (Birdsell et al., 2015). A portion (5–40 %) of the injected fracking fluid mixed with subsurface brine returns to the surface (flowback water) within the first 7–10 days from the injection. After this point, a slower flow of contaminated waters known as "produced water" resurfaces during the lifespan of a well (20–40 years). Environmental concerns caused by hydraulic fracturing are mainly related to water utilisation and wastewater treatment, including stress on the regional freshwater reserves and water pollution due to wastewater leakages (Agarwal and Kudapa, 2022). The significant water requirements of hydraulic fracturing can also increase the cost of freshwater in regions surrounding the well by up to 300 % (Ellafi et al., 2020). Therefore, wastewater treatment strategies aimed at the recovery of fracking wastewater could mitigate the stress on local freshwater resources, the risk of water pollution due to leakages from disposal sites and, possibly, reduce the prices of freshwater in regions surrounding the well.

In attempt to minimize the impacts and costs of hydraulic fracturing, various technologies, including membrane-based treatments, evaporation, coagulation, biological treatment and advanced oxidation processes (e.g. catalytic wet oxidation and ozonation), are being investigated (Sun et al., 2019). However, most of these technologies show limitations in the treatment of fracking wastewaters. For example, high iron oxide content in fracking wastewaters is a limiting factor for the use of membrane technologies due to fouling (Guo et al., 2018). Moreover, toxic contaminants dissolved in fracking wastewaters as well as the high ionic strength can deactivate microorganism and significantly reduce the effectiveness of biological treatment. Similarly, the presence of contaminants can lead to the passivation of electrodes during electrocoagulation, resulting in an inefficient removal of suspended salts, while the high energy use for evaporation leads to an increase in operating costs (Sun et al., 2019). Advanced oxidation processes, such as ozonation, are effective in the removal of COD from fracking wastewaters, but the presence of chlorine or bromine leads to the formation of chlorinated and brominated compounds of higher toxicity compared to their precursors (Lim et al., 2022). By contrast, catalytic wet oxidation (CWO) has been proven effective for the complete oxidation of toxic contaminants and can be utilised for the treatment of high ionic strength wastewaters without causing the formation of toxic by-products (Ou et al., 2022). It is also an effective method for the removal of organic contaminants from fracking wastewaters, reducing their chemical oxygen demand (COD) by 97 % (Liu et al., 2017).

Cerium oxides show good potential for the use in CWO of fracking wastewater. They are widely utilised in industrial applications, including advanced oxidation processes for water treatment due to their appealing redox properties, oxygen storage and transfer capacities, thermal stability and biocompatibility (Kurian, 2020). In particular, the oxygen storage and transfer capabilities of cerium oxide are very desirable properties for CWO applications due to the low solubility of oxygen in water (Ou et al., 2022). However, pure cerium oxides show poor catalytic activity for CWO and thus dopants, including other rare earth elements (e.g., Pr and La) and transition metal oxides, are incorporated into the cerium oxide lattice structure to form oxygen vacancies, enhancing oxygen mobility and the catalytic activity (Hammouda et al., 2017; Tsiotsias et al., 2022).

The utilisation of $MnCeO_x$ and other cerium-based mixed oxides for wastewater treatment have been widely reported (Arena et al., 2012; Kim and Ihm, 2011; Silva et al., 2004). In 1985, Imamura et al. demonstrated the effectiveness of $MnCeO_x$ (Mn/Ce = 7/3) in the wet oxidation of ammonia (Imamura et al., 1985), achieving a total nitrogen conversion of 69.9 % (Imamura et al., 1986). Complete oxidation of organic pollutants, including poly(ethylene glycol), acetic acid, *n*-butylamine and pyridine over $MnCeO_x$ catalyst was also investigated and total organic carbon (TOC) conversions up to 99.5 % were reported (Imamura et al., 1986). The remarkable activity of $MnCeO_x$ was attributed to an improved oxygen storage capacity and an enhanced oxygen mobility on the catalyst surface compared to those of single metal oxide catalysts due to the interaction between cerium and manganese (Chen et al., 2001). In addition, $MnCeO_x$ catalysts were proven to be resistant to chloride poisoning during CWO of phenol (Ou et al., 2022).

A Cu-Cr/activated carbon catalyst (10 g L^{-1}) was utilised in CWO for fracturing flowback fluid treatment at 250 °C under 2.5 MPa oxygen partial pressure, achieving a 97 % reduction in COD (Liu et al., 2017). It was also reported that copper oxide exhibits higher oxygen donation potential in oxidation reactions compared to manganese oxides (Matatov-Meytal and Sheintuch, 1998). Notably, the interaction between copper and cerium in $CuCeO_x$ catalyst can give rise to oxygen ion vacancies around copper ions, resulting in high activity for oxidation (Pintar et al., 2005). Overall, $CuCeO_x$ emerged as a promising catalyst in CWO of refractory organics in wastewater (Hočevar et al., 1999; Hočevar et al., 2000). Hence, $CuCeO_x$ could have the potential for the treatment of fracking wastewaters which have a high organic load, which has not been investigated previously.

Accordingly, this is the first study to compare the activities of $MnCeO_x$ and $CuCeO_x$ for CWO of synthetic fracking wastewater containing phenol (as a model compound of organic pollutants) in the presence of high concentration of NaCl (200 g L^{-1}) in a synthetic fracking wastewater (Warner et al., 2013). A further novelty of this work is that the environmental impacts of cerium-based CWO are quantified for the first time via life cycle assessment (LCA) in comparison to ozonation as a more mature technology. Moreover, the environmental impacts from the production of the two catalysts are also estimated for the first time as part of this work because these data are not available in literature or LCA databases.

2. Materials and methods

2.1. Catalyst synthesis and characterisation

Manganese (II) nitrate tetrahydrate ($Mn(NO_3)_2{\cdot}4H_2O$) was obtained from Alfa Aesar while other precursors, including cerium (III) nitrate hexahydrate ($Ce(NO_3)_3{\cdot}6H_2O$) and copper(II) nitrate trihydrate ($Cu(NO_3)_2{\cdot}3H_2O$), as well as phenol, were obtained from Sigma-Aldrich. Sodium hydroxide (NaOH) was obtained from Honeywell. All the chemicals were used as received.

$MnCeO_x$ and $CuCeO_x$ catalysts were synthesised by co-precipitation of aqueous manganese, copper and cerium nitrates with excess NaOH and the theoretical molar ratio of Mn/Ce or Cu/Ce was 1.5. To synthesise the catalysts, typically 9 mmol of manganese/copper nitrate and 6 mmol cerium nitrate were dissolved in 20 mL deionised water. Thereafter, 40 mL of 120 mM NaOH solution was added into the prepared solution dropwise

under vigorous stirring. The mixture was stirred for 30 min at room temperature to allow the precipitation of the desired binary metal oxide. The precipitate was separated from the aqueous phase by centrifugation and washed with deionised water to remove the excess NaOH until the wastewater achieved a pH value of about 7. The obtained precipitate was dried in an oven at 100 °C overnight and then calcined at 400 °C for 6 h in a muffle furnace.

The XRD patterns of the fresh catalysts were measured by a Bruker D2 Phaser benchtop X-ray powder diffractometer using Cu K_α radiation at 30 kV and 30 mA. The intensity data were collected in a 2θ range from 20° to 85° with a scan rate of 1° s^{-1} with a sample rotation rate of 20 rpm during the measurement. The molar ratio of Mn/Ce and Cu/Ce in the fresh catalysts were characterised by XRF (PANalytical MiniPal 4); metal content and distribution were measured by EDX elemental mapping with SEM (Quanta 250, beam acceleration voltage = 20 kV). N_2 physisorption analysis was carried out by a Micromeritics ASAP 2020, and the degas procedure was performed at 300 °C for 12 h prior to the adsorption. The redox properties of $MnCeO_x$ and $CuCeO_x$ catalysts were investigated via a QuantaChrom ChemBET Pulsar TPR/TPD Analyser. Reduction of the catalyst was carried out by passing 40 mL min^{-1} of H_2 (5 vol% in Ar) over the catalyst and increasing the catalyst temperature from room temperature to 750 °C at 10 °C min^{-1}. The XPS analysis of $CuCeO_x$ was performed according to the same experimental procedure as for the previously reported results for the $MnCeO_x$ catalyst (Ou et al., 2022). The results were obtained using a Kratos AXIS Ultra DLD apparatus equipped with a monochromated Al Kα X-ray source, a charge neutraliser, and a hemispherical electron energy analyser; $CuCeO_x$ powders were affixed to carbon-coated specimen holder before measurements. During data acquisition, the chamber pressure was kept below 10^{-9} mbar and a pass energy of 40 eV was used. The spectra were analysed using CasaXPS software and correction for charging was performed using the C 1s binding energy as the reference at 284.8 eV.

2.2. Catalytic wet oxidation

Synthetic phenolic wastewater was prepared using pure water to which an initial concentration of 1.0 g L^{-1} of phenol was added; this water was used for comparison with the synthetic fracking wastewater. The latter was prepared using the same initial phenol concentration as for the phenolic water, also adding 200 g L^{-1} of NaCl to simulate typical fracking wastewater. Catalysis tests (catalyst concentration: 1 and 5 g L^{-1}) were carried out in a CWO reactor (Parr stirred autoclave reactor, mode: 4598) filled with 50 mL of synthetic wastewater at 110 °C and 0.5 MPa O_2 partial pressure. The stirring speed in the CWO was set at 1800 rpm, and the catalysts were pelleted and sieved to select particles of size 63–95 μm with a low Weisz-Prater value (0.1) to ensure that the reaction was not mass-transfer limited. Details regarding the Weisz-Prater value calculation are reported in the Supporting Information (SI). Catalyst stability was investigated by performing a second CWO cycle. This involved reusing the used catalysts in the reaction system under the same reaction conditions as in the first cycle. The initial phenol concentration of the second cycle was kept at 1.0 g L^{-1} by adding more phenol into the reaction solution. All the experiments were repeated two times, and the deviation in the results was within 5 %.

The concentration of phenol and the intermediate products were measured by HPLC, while the organic carbon concentration was determined by a TOC analyser (TOC-VCSH, Shimadzu). Metal leaching was assessed by ICP-OES (PlasmaQuant PQ 9000 Elite, Analytic Jena) and the desorption properties of deposited carbon on the used catalysts were investigated by TPO-MS. Approximately 30 mg of the spent catalyst was exposed to O_2 (10 vol% in Ar) with a total flow rate of 100 cm^3 min^{-1} for 10 min at 100 °C before ramping the temperature up to 600 °C at a rate of 10 °C min^{-1}. Desorbed CO_2 was monitored using a Hiden Analytical HPR20 quadrupole mass spectrometer. The overall mass balance of the CWO process was estimated according to the abovementioned measurements and the results are reported in Table S1 in the SI.

2.3. Life cycle assessment

The LCA was conducted according to the ISO 14040/44 standards (ISO, 2006a; ISO, 2006b). The goal and scope of the study, inventory data and the impacts assessment method used in the study are described in the following sections. The interpretation of the findings is presented in the Results and Discussion section. The assessment followed the attributional approach and the GaBi 10.0 software was used for system modelling (Thinkstep, 2019).

2.3.1. Goal and scope definition

The main goal of this LCA was to assess the environmental impacts of treating fracking wastewater to remove the organic fraction by CWO in comparison to ozonation, with the aim of identifying benefits and drawbacks of CWO as well as improvement opportunities. The second goal was to estimate the impacts related to the production of Cu and Mn-based catalysts as these are not available in life cycle databases, to be able to identify the environmentally more sustainable catalyst for CWO.

The functional unit for the LCA of the catalysts was defined as '1 kg of catalyst produced'. For the wastewater treatment LCA, the functional unit was '1 m^3 of treated wastewater'.

A cradle-to-gate approach was considered for the production of metal catalysts (Fig. 1) as its utilisation and disposal are considered as part of the fracking wastewater treatment. As described in Section 2.1, metal nitrates are co-precipitated with NaOH in the co-precipitation step. The produced catalyst is then washed to remove impurities, dried and calcined.

A cradle-to-gate system boundary was also adopted for the assessment of the wastewater treatment, focusing on the removal of suspended solids (SS) and the complete oxidation of the organic fraction. The removal of SS was included within the system boundary as SS might block the access to the active sites of the catalyst, leading to its rapid deactivation. Two possible options were considered for the removal of SS prior to CWO: coagulation/flocculation and microfiltration (Fig. 2a & b, respectively). In the first option, aluminium sulphate is added to the wastewater, mixed, allowed to settle and then filtered. In the microfiltration option, the wastewater is filtered through a ceramic membrane before being sent to the catalytic reactor; this is followed by backwashing chemical cleaning.

The removal of SS was also considered as a preliminary step for the ozonation process, assuming the same two options as for CWO (Fig. 2c & d). Following the removal of the suspended solids, the ozonation process involves on-site production of ozone and its injection into the wastewater. Both CWO and ozonation produce wastewaters of comparable composition. Further details on the two types of treatment are provided in the following sections. Note that further treatment steps to lower the concentration of residual contaminants were not considered as they would be the same for both CWO and ozonation.

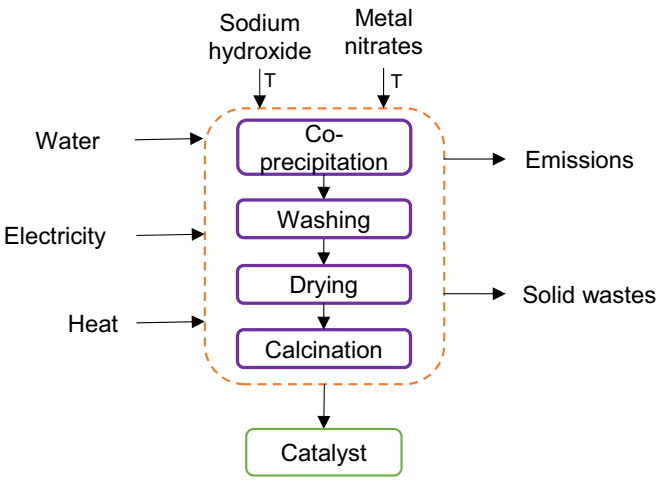

Fig. 1. System boundaries for the production of metal-based catalysts [T: transport].

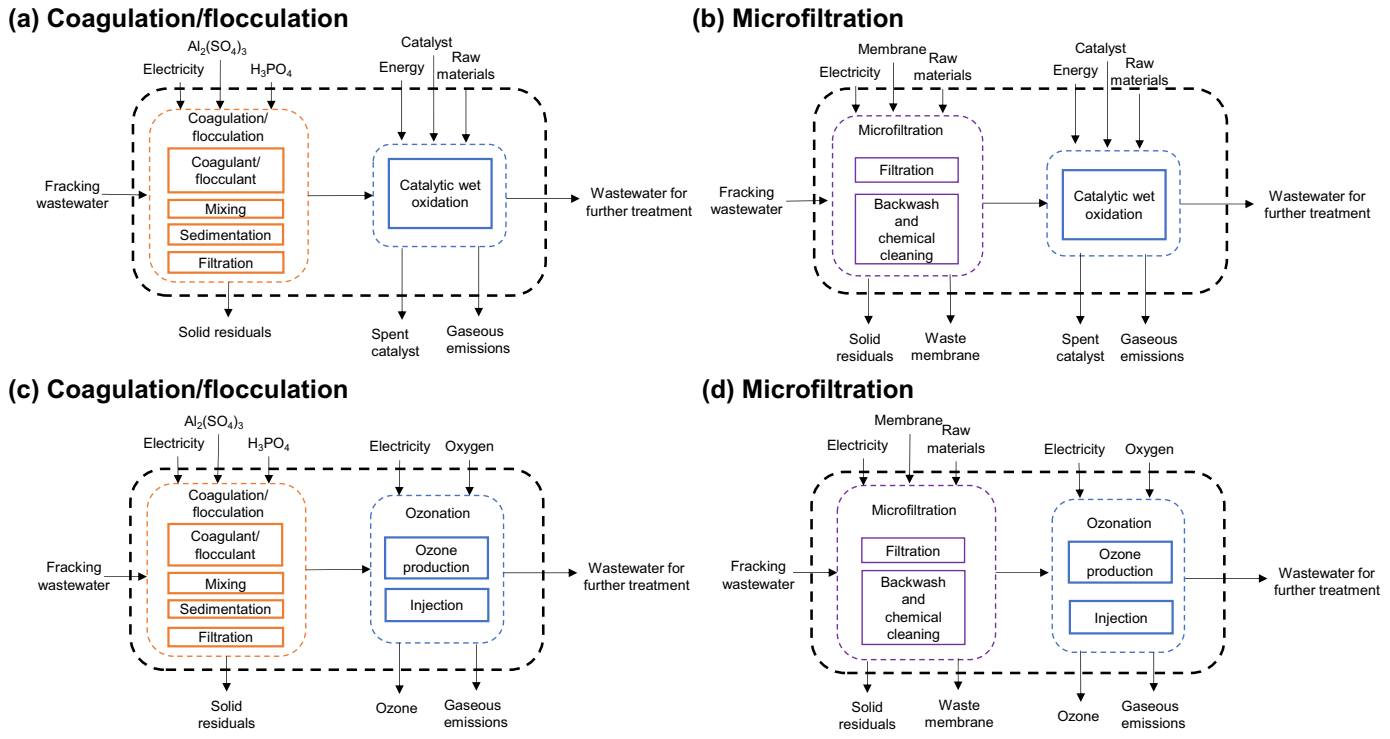

Fig. 2. System boundaries for catalytic wet oxidation (a & b) and ozonation (c & d) coupled with coagulation/flocculation or microfiltration.

2.3.2. Inventory data

Primary data on catalyst production were obtained from the experiment described in Section 2.1. Data on the wastewater treatment process for CWO and ozonation were sourced from literature and own estimates, as detailed further below. Background data for materials and energy were obtained from Ecoinvent 3.6, assuming that the treatment is based in the US (Wernet et al., 2016) due to the large-scale production of shale gas there and data availability. All background processes were adapted where needed to the US energy mix. Heat and electricity requirements for the treatment processes were estimated by correcting the theoretical energy requirements according to the scaling factors described in the literature (Cuellar-Franca et al., 2016) to scale up from laboratory to industrial-scale operations. Similarly, the energy used for mixing in both CWO and ozonation was estimated by applying scaling factors available in the literature (Piccinno et al., 2016). An average transportation distance of 100 km was considered for all materials and wastes. The inventory data are detailed on the following sections.

2.3.2.1. Catalyst production. The experiments described in Section 2.1 were utilised to estimate the amounts of materials required for the preparation of the catalysts (Table 1). A theoretical Mn/Ce and Cu/Ce ratio of 1.5, consistent with the results of XRF analyses reported in Section 3.1, was considered for the LCA models. For NaOH, a 20 % excess (0.9 kg per kg catalyst) on the theoretical amount added to the solution was assumed to ensure the precipitation of the metal phase. The theoretical amount of NaOH utilised by the process was estimated stoichiometrically (2 mols of NaOH react with 1 mol of $Cu(NO_3)_2$ or $Mn(NO_3)_2$ and 3 mols of NaOH react with 1 mol of $Ce(NO_3)_3$). NaOH used in the catalysts synthesis was assumed to be recovered from the process water (at a 44 % recovery rate) by electrodialysis (Imran et al., 2015) and reused in the process. Consequently, the consumption of 0.5 kg NaOH per kg catalyst was assumed. However, the amount of NaOH which would be utilised at industrial scale is uncertain. Therefore, a sensitivity analysis was performed (Section 3.3.1) to determine the effect on the impacts of catalyst preparation using the theoretical and amount of NaOH and the excess used in the laboratory

Table 1
Inventory data for the production of $CuCeO_x$ and $MnCeO_x$ catalysts.

Reagents/wastewater	Item[a]	Quantity		Unit (per kg of catalyst)	Comments
		$CuCeO_x$	$MnCeO_x$		
Reagent	$Cu(NO_3)_2$	1.1	–	kg	Produced via conventional route: reaction of elemental copper with nitric acid
	$Mn(NO_3)_2$	–	1.1	kg	Produced via conventional route: reaction of manganese oxide with nitric acid
	$Ce(NO_3)_3$	1.3	1.3	kg	Produced via reaction of quadrivalent cerium hydroxide and nitric acid in presence of hydrogen peroxide (Pitts, 1979)
	NaOH	0.5	0.5	kg	
	Water	19.7	19.7	kg	
	Heat	606	756	kJ	
	Electricity	2.2	2.2	Wh	
Wastewater[b]	Nitrates	4.3	4.3	g	
	Copper	9.4	–	mg	
	Manganese	–	92.1	mg	
	Sodium	0.2	0.2	kg	

[a] Life cycle inventory data sourced from Ecoinvent 3.6 (Wernet et al., 2016).
[b] Residual concentration, estimated after wastewater treatment.

experiments (0.7 and 2.4 kg per kg of catalyst added to the solution, respectively, with a consumption of 0.4 and 1.3 kg per kg catalyst).

According to the literature data (Piccinno et al., 2016), the electricity for stirring used during the preparation of the two catalysts was estimated at 2.2 Wh kg^{-1} catalyst, as comparable amounts of reagents are required for the production of the same amounts of the two catalysts. On the contrary, their heat requirements differ (Table 1) due to the different heat capacities of their respective reagents.

Wastewater produced during the catalyst synthesis was assumed to be processed in a medium-size wastewater treatment plant (capacity class 3) due to the presence of toxic substances (see Table 1). Owing to a lack of specific data, treatment of wastewater from mineral oil storage was considered as a proxy due to the similarities in pollutants content (Wernet et al., 2016). The impacts of the water treatment were included in the study, but the impacts of treated water discharged into the environment were out of scope.

2.3.2.2. Fracking wastewater treatment. A wastewater flow rate of 46 L h^{-1} was estimated according to a volume of ~16,000 m^3 per well resurfacing during the well's lifetime (40 years). This value was used to estimate the energy consumption of coagulation and microfiltration, as well as the membrane area and the amount of catalyst required by the treatment processes. The average composition of the fracking wastewater assumed in the study can be found in Table 2. This is based on Marcellus Shale wastewaters as this shale play contains 87 % of the total shale gas available in the Northeast region of the US and 55 % of the total onshore shale gas in the country (INTEK, 2011). Note that the salinity and organic carbon content of the synthetic fracking wastewater described in Section 2.2, which utilised phenol as a model compound, are representative of those reported for Marcellus Shale wastewaters (Al-Ghouti et al., 2019; He and Vidic, 2016; Lee and Neff, 2011). Accordingly, it is assumed that the performance of the catalysts for the treatment of Marcellus Shale wastewaters would be comparable to those reported for the synthetic fracking wastewater considered here.

The assumed concentration of suspended solids was also representative of the concentrations found in the fracking wastewater (Table 2). Their removal was included in the LCA modelling since it is part of common fracking wastewater treatment as mentioned in Section 2.3.1. The concentration of the suspended solids was utilised to estimate the materials and energy required by the coagulation and microfiltration processes used for their removal. The other contaminants given in Table 2 were included in the models because they also affect the amount of reagents utilised for the wastewater treatment. Specifically, coagulants reduce the alkalinity of the wastewater, while ozone tends to react with dissolved iron and manganese (Hussain et al., 2022). The COD of the fracking wastewater was considered to represent the total organics concentration and was utilised to determine the total amount of catalyst or ozone required by the treatment processes. The US energy (heat and electricity) mix was considered for all models and fracking wastewater from the Marcellus Shale (the largest reserve of shale gas in the US) was selected in this study as the US is the largest producer of shale gas internationally. Detailed descriptions of the processes considered and related assumptions are provided in the following sections, starting with the pre-treatment to remove the suspended solids and followed by the removal of organics by either CWO or ozonation.

Table 2
Assumed composition of the fracking wastewater.

Contaminant	Quantity (g m^{-3} treated wastewater)[a]
Total suspended solids	1184
COD	26,173
Fe	4029
Mn	437
Alkalinity	143

[a] Average composition of Marcellus Shale wastewater (Al-Ghouti et al., 2019; He and Vidic, 2016; Lee and Neff, 2011).

2.3.2.2.1. Pre-treatment to remove suspended solids. As mentioned in Section 2.3.1, two options were considered for the removal of suspended solids: i) coagulation; and ii) microfiltration.

i) *Coagulation*: This process involves rapid and slow mixing, sedimentation and rapid sand filtration. The inventory data are summarised in Table 3.

Aluminium sulphate was selected as one of the most common coagulants utilised in water treatment (Adebayo et al., 2021; Barrios et al., 2008; Lapointe et al., 2021). The amount of coagulant utilised was calculated according to the turbidity of the wastewater (Takić et al., 2019):

$$\text{Turbidity (NTU)} = 2.511 - 0.162X + 0.003X^2 \quad (1)$$

where X is the amount of aluminium required in ppm and NTU represents nephelometric turbidity units. Turbidity is also correlated with concentration of suspended solids as follows (Serajuddin et al., 2019):

$$\text{Turbidity (NTU)} = \frac{\text{Total suspended solids (ppm)}}{0.3747} - 1.3598 \quad (2)$$

Given the concentration of suspended solids in the wastewater of 1184 ppm (Table 2), the turbidity of wastewater is equal to 3157 NTU and, thus, 247 g m^{-3} of aluminium sulphate is required for coagulation. Moreover, removal of the alkaline fraction of the wastewater considered requires additional 14.2 g m^{-3} treated wastewater, hence the total consumption of the coagulant is 261 g m^{-3} (Table 3). Note that the organic fraction would also be affected by the coagulation process, as intake of organic carbons in flocs is commonly observed (Chorghe et al., 2017). However, low COD removal efficiencies (<20 %) are reported for the coagulation of fracking wastewaters (Jin et al., 2018; Sun et al., 2019). Moreover, process optimisation with respect to the coagulant and operating conditions is necessary to achieve the expected removal efficiencies. As the optimisation of the coagulation process for the removal of the organic fraction is beyond the scope of this study, this process was considered only as a means to remove suspended solids from the wastewater.

Additional materials required for the maintenance of sand filters include phosphoric acid for chemical washing and water for backwashing (6.4 mg and 68 mL m^{-3} treated wastewater, respectively) (Barrios et al., 2008). Solid residues produced by the process (1.4 kg m^{-3} treated wastewater) are considered hazardous waste and were assumed to be disposed in hazardous-waste landfill.

The total energy requirements (0.12 kWh m^{-3} treated wastewater) were estimated based on the expected wastewater flow rate (46 L h^{-1}) and the mixing and filtration (including backwashing) energy requirements reported in the literature (Barrios et al., 2008; Vadasarukkai and Gagnon, 2017).

ii) *Microfiltration*: This technology is widely utilised for the removal of suspended solids of sizes >1 μm in various applications, including fracking wastewater treatment (Sun et al., 2019). Among different membranes investigated for the treatment of fracking wastewaters from Marcellus Shale, ceramic membrane emerged as an effective option due to their higher resistance to fouling and corrosion, as well as better thermal stability and mechanical strength compared to polymeric membranes (Hakami et al., 2020; He and Vidic, 2016). Accordingly,

Table 3
Inventory data for the coagulation process.

Process	Item[a]	Quantity	Unit (per m^3 of treated wastewater)
Inputs	Aluminium sulphate	261	g
	Electricity	0.12	kWh
	Phosphoric acid	6.4	mg
	Water	68	mL
Outputs	Solid waste	1.4	kg

[a] Life cycle inventory data sourced from Ecoinvent 3.6 (Wernet et al., 2016).

Table 4
Inventory data for the microfiltration process.

Process	Item[a]	Quantity	Unit (per m^3 of treated wastewater)
Inputs	Membrane (aluminium oxide)	11.4	cm^2
	Electricity[a]	0.41	kWh
	NaOH	301	mg
Outputs	Solid waste[a]	1.2	kg

[a] Suspended solids. Life cycle inventory data sourced from Ecoinvent 3.6 (Wernet et al., 2016).

aluminium oxide membranes were considered as a filter medium in this study. The total surface area of the membrane (2.3 m^2) was estimated according to an operating flux of 20 L m^{-2} h^{-1} (wastewater flow rate: 46 L h^{-1}), as lower fluxes tend to increase the operating costs (Tangsubkul et al., 2006). The manufacturing data for membrane modules were based on LCA databases and literature data (Tangsubkul et al., 2006; Wernet et al., 2016), adapted for the use of aluminium oxide (Table S2 in the SI). Electricity requirements of the process (0.41 kWh m^{-3} treated wastewater) were estimated according to a transmembrane pressure of 70 kPa, a backwash frequency of 1 cycle per hour (Basu, 2015; He and Vidic, 2016). Furthermore, it was considered that chemical cleaning using NaOH (301 mg m^{-3} treated wastewater) would be performed every 10 days to prevent membrane fouling (Parameshwaran et al., 2001). As discussed in Section 2.3.2.3, solid residuals were considered as hazardous wastes and disposed by landfill. The membrane lifetime was assumed at five years (Tangsubkul et al., 2006). The inventory data for the microfiltration process are summarised in Table 4.

2.3.2.2.2. Catalytic wet oxidation. Experimental observations on the catalyst performance reported in Section 3.2 were utilised to model the CWO treatment process at commercial scale. Only the Mn-based catalyst was considered for LCA modelling as the Cu-based alternative showed poor activity (~63 % TOC removal), which would not achieve the TOC concentration required for water reuse as fracking fluid or for other production activities (Sun et al., 2019). It should be noted that the dissolved iron, one of the contaminants in fracking wastewaters (Table 2), might also react with the organic fraction, possibly increasing the effectiveness of the catalysts above the catalytic activity considered (Esteves et al., 2022; Kaldas et al., 2020). However, no experimental observations quantifying the promoting effect of dissolved iron on CWO of fracking wastewaters are currently available. Thus, its potential effect on the catalytic activity was not included as part of this assessment. Nonetheless, dissolved iron was considered as one of the contaminants which affects the amount of ozone required for the ozonation-based treatment (Section 2.3.2.2.3). It should also be borne in mind that the catalyst was tested by utilising phenol as a model molecule. Hence, it was assumed that the whole organic fraction would behave as pure phenol. This assumption was made as the activity of the catalysts in a more complex organic matrix, which might cause competitive effects and, possibly, lead to lower catalytic activity, is currently unknown.

Based on the average wastewater flow rate reported in Section 2.3.2.2.1 (46 L h^{-1}) and on COD concentration of 26,173 g m^{-3} wastewater, it was estimated that the catalytic reactor would require 12 kg of catalyst. According to an average catalyst lifetime of three years (Argyle and Bartholomew, 2015), a catalyst consumption of 10 g m^{-3} treated wastewater was estimated (Table 5), with the waste catalyst landfilled. However, the lifetime of catalysts considered by this study is currently unknown as they are in their early development stages. Therefore, a sensitivity analysis, which considered shorter (0.5 years) and longer (five years) lifetime was conducted to determine the effect on the CWO process.

Temperatures of about 200 °C have been reported for fracking wastewaters from deep shales (3200–4100 m) in southern regions of the US (Kahrilas et al., 2016). Such temperatures would allow operating the CWO process without the aid of external heating sources. However, downhole water temperatures in shallower wells (<1200 m) can fall down to 40–100 °C (King, 2008). Moreover, as wells tend to experience pressure and temperature cycles during operation, water temperature can be as low as 18 °C (EPA, 2016). Accordingly, an average wastewater temperature of 70 °C was considered, which would require 706 MJ_{th} m^{-3} treated wastewater to reach the process operating temperature (110 °C). However, the effect of lower (18 °C, requiring 1.6 GJ_{th} m^{-3} treated wastewater) and higher temperatures (200 °C, no heat requirements) was considered in a sensitivity analysis. Note that for wastewater temperature higher than the operating temperature of CWO (110 °C) no external heat sources would be required by the process. Moreover, higher reaction temperatures might increase the COD removal (Bhargava et al., 2006). However, the effect of higher reaction temperatures on the catalytic activity was not included as part of the assessment due to the lack of experimental data.

Table 5
Inventory data for the catalytic wet oxidation process.

Process	Item[a]	Quantity	Unit (per m^3 of treated wastewater)
Inputs	Catalyst	10	g
	Heat (natural gas)	706	MJ_{th}
Outputs	Carbon dioxide	68.8	kg
	Residual COD	1.7	kg
	Manganese leaching	12.6	mg
	Spent catalyst	10	g

[a] Life cycle inventory data sourced from Ecoinvent 3.6 (Wernet et al., 2016).[b]

A residual COD content of 1.7 kg m^{-3} treated wastewater was estimated according to Eq. (3) (Dubber and Gray, 2010), based on the TOC removal rate of 94 % (for the latter, see Section 3.2):

$$COD = 49.2 + 3 \text{ x } TOC) \quad (3)$$

Moreover, CWO also releases 68.8 kg CO_2 m^{-3} treated wastewater from the complete oxidation of the organic fraction and 12.6 mg Mn m^{-3} treated wastewater due to metal leaching (0.52 wt%), as reported in Section 3.2.

2.3.2.2.3. Ozonation. Ozone is a powerful oxidant utilised in various industrial processes, including water treatment (Aguilar-Alarcón et al., 2022), chemical synthesis (Phung Hai et al., 2022), agriculture (Botondi et al., 2021) and gaseous pollutants control (Lin et al., 2020). Due to its instability, ozone is produced in situ via electrical discharge utilising oxygen as the feedstock (Ikehata and Li, 2018). In recent years ozonation was also proven to be effective for the removal of COD, colour and phenol from fracking wastewater (Sun et al., 2019). Nevertheless, the possible formation of chlorinated or brominated by-products of reaction, which might be more hazardous than their precursors, is a cause of concern in the treatment of high-salinity wastewaters. However, direct observations are required to determine the type and concentration of these hazardous by-products. Thus, due to a lack of data, this possible effect was not considered in this study.

Inventory data for the ozonation process are provided in Table 6. According to literature data on ozonation of several wastewaters, including

Table 6
Inventory data for the ozonation process.

Process	Item[a]	Quantity	Unit (per m^3 of wastewater)
Inputs	Oxygen[b]	561	kg
	Electricity	1.1	MWh
	Cooling water	1108	kg
Outputs	Carbon dioxide	73.3	kg
	Solid waste (FeOH and MnO_2)	8.4	kg
	Cooling water	1108	kg

[a] Life cycle inventory data sourced from Ecoinvent 3.6 (Wernet et al., 2016).
[b] For on-site generation of ozone.

fracking wastewaters (Lim et al., 2022; Nijdam et al., 1999), it was considered that the oxidation process requires 2.5 g O_3 g^{-1} COD. This is a conservative assumption as a lower amount of ozone would be required if the treatment was limited to the oxidation of phenol (2.1 g O_3 g^{-1} phenol are required) in the pH range of fracking wastewaters (Gould and Weber, 1976; Joshi and Shambaugh, 1982). Based on the assumed COD of the fracking wastewater (Table 2), 65.4 kg O_3 m^{-3} treated wastewater is required. Ozone also reacts with dissolved iron, reducing Fe(II) to Fe(III), which hydrolyses to $Fe(OH)_{3(s)}$, and with manganese, which is oxidised from Mn(II) to $MnO_{2(s)}$. Produced particulates are commonly removed by filtration. Based on the reaction stoichiometry, it was estimated that 1.8 and 0.3 kg O_3 m^{-3} treated wastewater would be required for the removal of dissolved Fe and Mn, respectively. Energy (1.1 MWh m^{-3} wastewater) and materials required for the production of O_3, including oxygen and cooling water (561 and 1108 kg m^{-3} wastewater, respectively), were calculated according to literature and Ecoinvent data (Munoz et al., 2009; Wernet et al., 2016), while the amount of CO_2 generated by the oxidation of the organic fraction (73.3 kg m^{-3} wastewater) was determined stoichiometrically. Similarly, the amount of solid waste produced, including Fe $(OH)_2$ (7.7 kg m^{-3} wastewater) and MnO_2 (691 g m^{-3} wastewater) was also calculated stoichiometrically, based on Fe and Mn concentrations in the wastewater (Table 2). It should be noted that the formation of by-products of reaction is expected during ozonation of phenols and other organic compounds (Barlak et al., 2020; Xiong et al., 2020; Zhou et al., 2020). However, similar to chlorinated and brominated by-products, the type and amount of by-products are strongly influenced by the reaction conditions and wastewater composition due to the complex reaction mechanisms and kinetics involved (Lim et al., 2022). Thus, direct observations are required to determine if by-products are formed during the ozonation step and at what concentrations. Further treatment steps might be required to remove the by-products formed during this treatment step. These were not considered due to a lack of data.

2.3.3. Life cycle impact assessment

The life cycle impacts were estimated by applying the ReCiPe 2016 V1.1 impact assessment method at the mid-point level, following the hierarchist approach (Huijbregts et al., 2016).

All 18 impact categories included in this version of ReCiPe were considered, as follows: climate change (CC), fossil depletion(FD), metals and minerals depletion (MMD), water depletion (WD), human toxicity cancer & non-cancer (HTc & HTnc), freshwater (FET), marine (MET) and terrestrial ecotoxicity (TET), freshwater (FE) and marine eutrophication (ME), land use (LU), terrestrial acidification (TA), particulate matter formation (PMF), photochemical ozone formation ecosystems & human health (POFe & POFh), ozone depletion (OD) and ionizing radiation (IR).

3. Results and discussion

3.1. Catalyst characterisation

XRD patterns of $MnCeO_x$ and $CuCeO_x$ catalysts are shown in Fig. 3a. As expected, diffraction peaks of CeO_2 were observed in both catalysts. Moreover, manganese oxides with different oxidation states (2θ = 37.0°, 38.2°, 65.1°, 66.2°, 69.8° and 77.5°) (Bah, 2013) were observed in the $MnCeO_x$ catalysts, whilst crystalline CuO was clearly observed in the $CuCeO_x$ catalysts (2θ = 35.53° and 38.75°) (Hou et al., 2022; Lamonier et al., 1996; Papadopoulos et al., 2022; Tadjarodi and Roshani, 2014). Compared to the $MnCeO_x$ catalysts, the addition of copper in the $CuCeO_x$ catalysts led to the formation of a more amorphous CeO_2, as demonstrated by the broadening ceria peaks located at 28.6°, 33.3°, 47.5°, and 56.5° 2θ, respectively. Both $MnCeO_x$ and $CuCeO_x$ catalysts are mesoporous, as demonstrated by the type IV adsorption-desorption isotherms with a H3 hysteresis loop (Fig. 3b) and show a narrow pore size distribution, with 6 nm pores being dominant on $MnCeO_x$ and 4 nm pores on $CuCeO_x$ (Fig. S1). The BET surface areas of $MnCeO_x$ and $CuCeO_x$ catalysts were 191.5 and 108.7 m^2 g^{-1}, respectively. The larger surface area and pore size of $MnCeO_x$ allows easier accesses for phenol to the active sites and, thus, it may promote catalytic activities.

The elemental analysis of $MnCeO_x$ and $CuCeO_x$ shown in Fig. 4 shows the uniform metal distribution of the considered active phases in the two cerium-based mixed oxides. The Mn/Ce atomic ratio in $MnCeO_x$ was ~1.3 and the Cu/Ce atomic ratio in $CuCeO_x$ was ~1.7. The XRF tests further confirmed that the Mn/Ce and Cu/Ce ratio in the catalysts were ~ 1.4 and ~ 1.5; this was consistent with the theoretical value (i.e. 1.5) considered in the LCA models (Section 2.3.2.1).

The TPR profiles of $MnCeO_x$ and $CuCeO_x$ catalysts are shown in Fig. 5 with a two-step reduction profile observed for both catalysts. The reduction temperatures of $MnCeO_x$ were 349 and 444 °C, where the peak at 349 °C was attributed to the reduction of MnO_2/Mn_2O_3 to Mn_3O_4, while the high-temperature peak corresponded to the reduction of Mn_3O_4 to MnO, as well as the reduction of surface cerium (de Lima et al., 2022; Tang et al., 2006). Notably, results of the TPR analysis showed the presence of Mn with different oxidation states in $MnCeO_x$, which was consistent with the XPS analysis (both Mn^{3+} and Mn^{4+} were present with Mn^{3+} as the predominant oxidation state on the $MnCeO_x$ surface) (Ou et al., 2022). Regarding $CuCeO_x$, the low-temperature (235 °C) reduction peak was attributed to highly dispersed CuO, whereas the high-temperature (306 °C) peak attributed to bulk CuO, as established by the previous studies (Papavasiliou et al., 2022). The results of the XPS analysis also showed that Cu^{2+} was the main oxidation state of Cu on the surface of $CuCeO_x$ (Fig. S2). These findings are consistent with the results from the XRD analysis, which showed the presence of bulk CuO in $CuCeO_x$. In regard to cerium oxides,

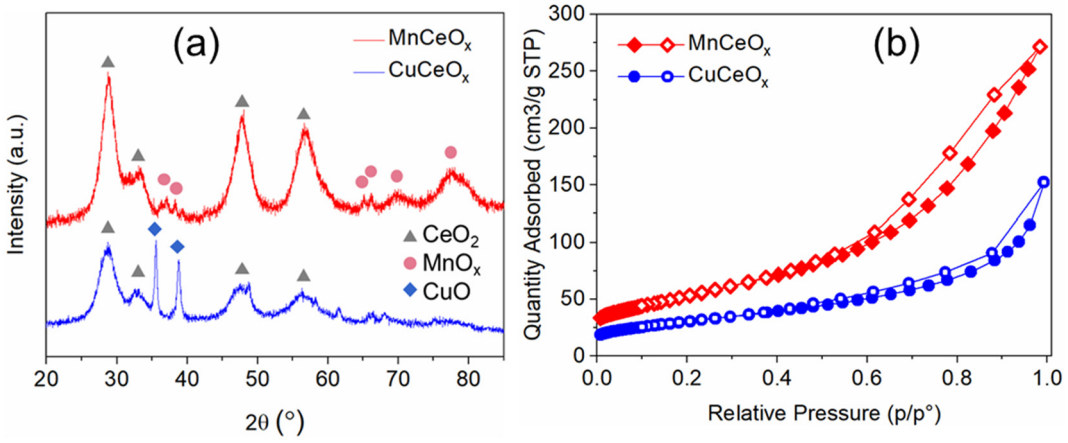

Fig. 3. XRD patterns (a) and N_2 sorption isotherms (b) of the $MnCeO_x$ and $CuCeO_x$ catalysts.

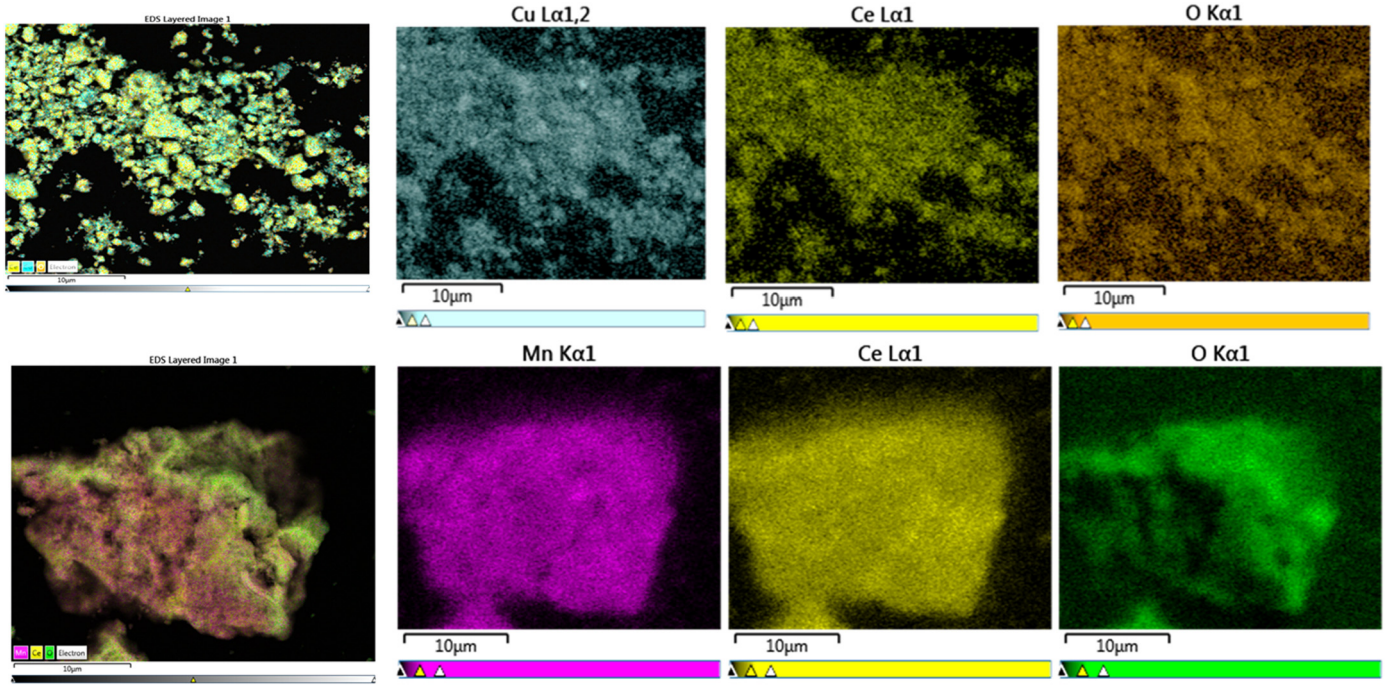

Fig. 4. SEM-EDS maps of the $CuCeO_x$ (top) and $MnCeO_x$ (bottom) catalysts.

results of the XPS analysis clearly showed that the surface chemical state of cerium is Ce^{4+} for both $MnCeO_x$ and $CuCeO_x$.

3.2. Catalyst activity and stability

The catalytic performance of $MnCeO_x$ and $CuCeO_x$ (1 g L^{-1}) is illustrated in Fig. 6. Notably, $MnCeO_x$ gave higher phenol (38.4 % vs. 6.8 %) and TOC removals (37.5 % vs. 5.9 %) compared to $CuCeO_x$, during catalytic tests carried out in the phenolic wastewater. In contrast, $CuCeO_x$ showed higher phenol removal than $MnCeO_x$ (65.4 % vs. 43.8 %) during tests conducted in the synthetic fracking wastewater. However, a lower TOC removal was observed during these tests for $CuCeO_x$ (32.7 % vs. 42.0 % for $MnCeO_x$), which was likely caused by Cu^{2+} ions leaching from the catalyst (Alejandre et al., 1998; Arena et al., 2003; Matatov-Meytal and Sheintuch, 1998) in the presence of high concentration of NaCl (200 g L^{-1}), as described below.

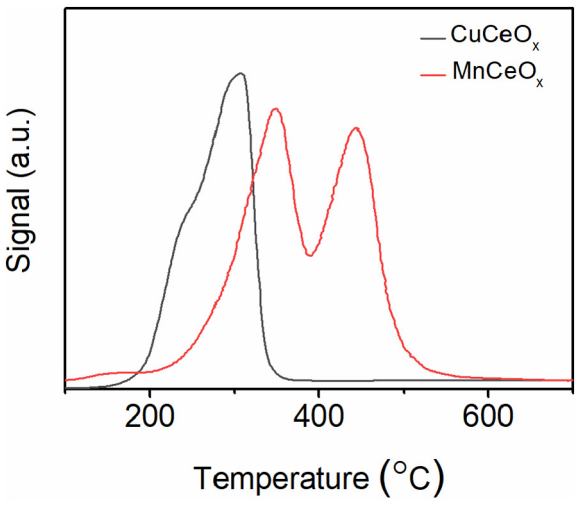

Fig. 5. TPR profiles of $MnCeO_x$ and $CuCeO_x$.

As reported in Table 7, an increase in the catalyst concentration to 5 g L^{-1} allowed complete phenol removal to be achieved over $MnCeO_x$ in both the phenolic and fracking wastewaters, with TOC removals of about 94 % in both wastewaters. Similarly, the phenol and TOC removals over $CuCeO_x$ (at 5 g L^{-1}) increased compared to that observed at 1 g L^{-1} catalyst concentration for both phenolic wastewater (23.3 % and 20.5 % vs 6.8 % and 5.9 %, respectively) and synthetic fracking wastewater (69.1 % and 63.0 % vs 65.4 % and 32.7 %, respectively). Overall, the activity of $CuCeO_x$ catalysts was lower compared to that of the $MnCeO_x$ catalysts for the treatment of both wastewaters considered. Thus, these tests demonstrated that $MnCeO_x$ is a more effective catalyst for complete removal of phenol in wastewaters.

Stability tests (two CWO cycles) of the $MnCeO_x$ and $CuCeO_x$ catalysts (at concentration of 1 g L^{-1}) for phenol and TOC removals are presented in Fig. 6. Notable decreases in phenol and TOC removals were observed for $MnCeO_x$, in both phenolic wastewater (from 38.4 % to 8.0 % and from 37.5 % to 7.9 % for phenol and TOC removal, respectively) and fracking wastewater (from 43.8 % to 23.8 % and from 41.0 % to 20.7 % for phenol and TOC removal, respectively). With respect to $CuCeO_x$, comparable catalytic activity was observed during the two reaction cycles in phenolic wastewater (from 6.8 % to 5.0 % and from 5.9 % to 4.9 % for phenol and TOC removals). Similarly, comparable phenol removal rates were observed during stability tests in synthetic fracking wastewater (65.4 % and 64.5 % for the first and second cycle); however, the TOC removal decreased from 32.7 % in the first cycle to 16.7 % in the second cycle. Significant concentrations of *p*-benzoquinone (87.3 mg L^{-1} in the first cycle and 158.6 mg L^{-1} in the second cycle) were detected during the stability tests of $CuCeO_x$ in fracking wastewater (Fig. S3), which could be attributed to copper leaching, as reported in previous studies (Alejandre et al., 1998).

Overall, $MnCeO_x$ showed high activity for the removal of TOC (94.0 %) during the first reaction cycle, emerging as a promising catalyst for CWO of fracking wastewaters, while $CuCeO_x$ was less suitable for this application. Notably, both catalysts showed significant activity losses during a second CWO cycle and, in the case of $CuCeO_x$, significant metal leaching was also observed. Accordingly, no additional CWO cycles were performed as part of this study.

To confirm whether copper leaching was the main reason for the low TOC removal of $CuCeO_x$ in the synthetic fracking wastewater, metal

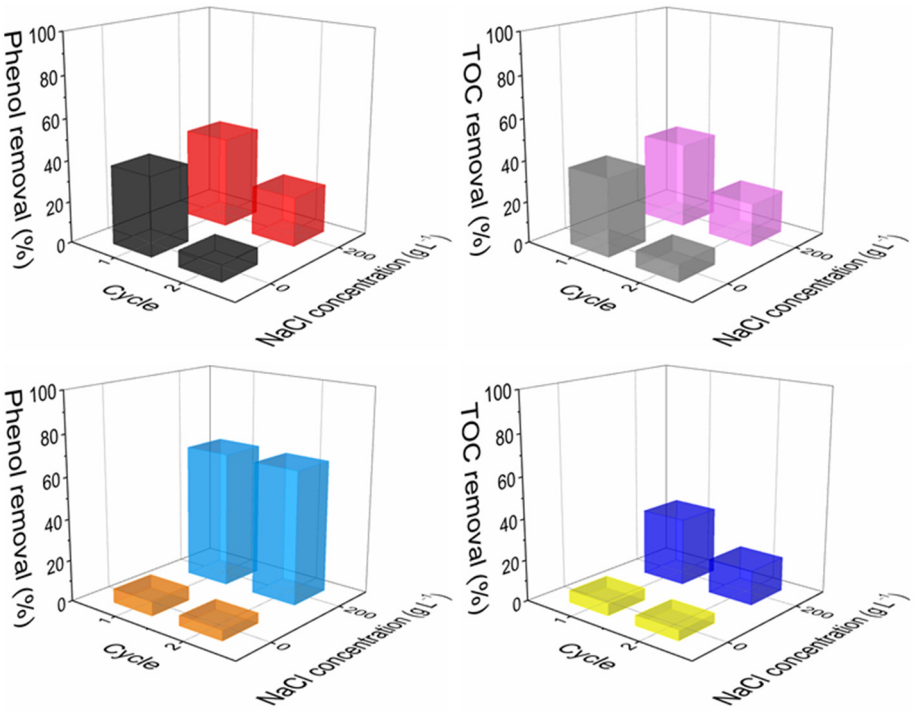

Fig. 6. Stability evaluation of $MnCeO_x$ (top) and $CuCeO_x$ (bottom) catalysts in CWO of phenolic and fracking wastewater (conditions in each cycle: $C_{phenol} = 1\ g\ L^{-1}$, $P_{O_2} = 0.5$ MPa, $C_{catalyst} = 1\ g\ L^{-1}$, $t = 2$ h). The experimental error is within 5 %.

concertation was examined after the two CWO cycles. Although negligible metal leaching of $CuCeO_x$ was measured in phenolic wastewater, 27 wt% and 55 wt% copper leaching were observed in the first and second CWO cycle, respectively, during stability tests in the synthetic fracking wastewater. The severe copper leaching was caused by the presence of high concentration of NaCl, which is known to promote copper leaching from copper ore minerals (Senanayake, 2007). Although the effect of NaCl on copper leaching from $CuCeO_x$ catalysts is still under investigation, it is currently assumed that chloride ions enabled the copper leaching by a Cu(I)/Cu(II) redox couple which shows large mixed potentials (Carneiro and Leão, 2007; Senanayake, 2007). On the contrary, negligible metal leaching was found for $MnCeO_x$ during the two CWO cycles in both phenolic and fracking wastewater. No cerium leaching was detected from either catalyst.

The used catalysts were characterised by TPO-MS, as detailed in Table 8. The quantity of carbonaceous deposits on the surface of the used $MnCeO_x$ catalyst in the synthetic fracking wastewater was ~45 % lower than that in the phenolic wastewater (9.9 and 17.7 mmol g^{-1}, respectively), which suggested that the presence of NaCl partially prevented coke formation on the catalyst surface, avoiding the loss of activity observed during the second cycle in phenolic wastewaters. On the contrary, the carbonaceous deposit over the surface of the used $CuCeO_x$ catalyst almost tripled in the fracking wastewater. The activity data together with the results from ICP analyses suggested that the higher phenol removal in the synthetic fracking wastewater was mainly caused by the catalytic effect of leached copper ions from the $CuCeO_x$ catalyst, driving mostly phenol conversion to polymerisation products, which are more stable compared to phenol and, thus, resistant to further oxidation (Arena et al., 2003).

3.3. Life cycle environmental impacts

Life cycle environmental impacts related to the production of the metal catalysts are discussed first, followed by the assessment of CWO in comparison with ozonation and sensitivity analyses for CWO.

3.3.1. Catalyst production

The cradle-to-gate environmental impacts of catalysts are shown in Fig. 7. As can be seen, the $MnCeO_x$ catalyst has lower impacts per kg catalyst (11–98 %) than the Cu-based alternative for 17 out of 18 categories. This is due to the use of manganese nitrate, which has 40–99 % lower impacts compared to copper nitrate but leads to a 162 % higher ionizing radiation. As a result, the latter is 65 % higher for the Mn-based than for the Cu-based catalyst.

The nitrate precursors used for the production of the two catalysts are the main contributors to the impacts, with cerium nitrate accounting for 2–93 % in both catalysts, copper nitrate 29–98 % in $CuCeO_x$ and manganese nitrate 7–64 % in $MnCeO_x$. Their impacts are due to the burdens from extraction and processing of the respective metal (Wernet et al., 2016). NaOH consumption also has a significant contribution to climate change (15 %), marine (16 %) and terrestrial ecotoxicity (49 %), freshwater (12 %) and marine eutrophication (17 %) for $MnCeO_x$, while in $CuCeO_x$ it is significant only for climate change (12 %) due to the more impacts of

Table 7
Phenol and TOC removals over $MnCeO_x$ (conditions: $C_{phenol} = 1.0\ g\ L^{-1}$, $C_{catalyst} = 5.0\ g\ L^{-1}$, $T = 110$ °C, $P_{O_2} = 0.5$ MPa, $t = 2$ h).

	$MnCeO_x$		$CuCeO_x$	
	NaCl concentration (g L^{-1})			
	0	200	0	200
Phenol removal (%)	100.0	100.0	23.3	69.1
TOC removal (%)	94.0	94.0	20.5	63.0

Table 8
TPO-MS data of used $MnCeO_x$ and $CuCeO_x$ catalysts (conditions: $C_{phenol} = 1\ g\ L^{-1}$, $P_{O_2} = 0.5$ MPa, $C_{catalyst} = 1\ g\ L^{-1}$, $t = 2$ h).

	$MnCeO_x$		$CuCeO_x$	
	Temperature (°C)	CO_2 Production (mmol g^{-1})	Temperature (°C)	CO_2 Production (mmol g^{-1})
No NaCl	374	17.7	263	6.0
With NaCl	410	9.9	383	19.5

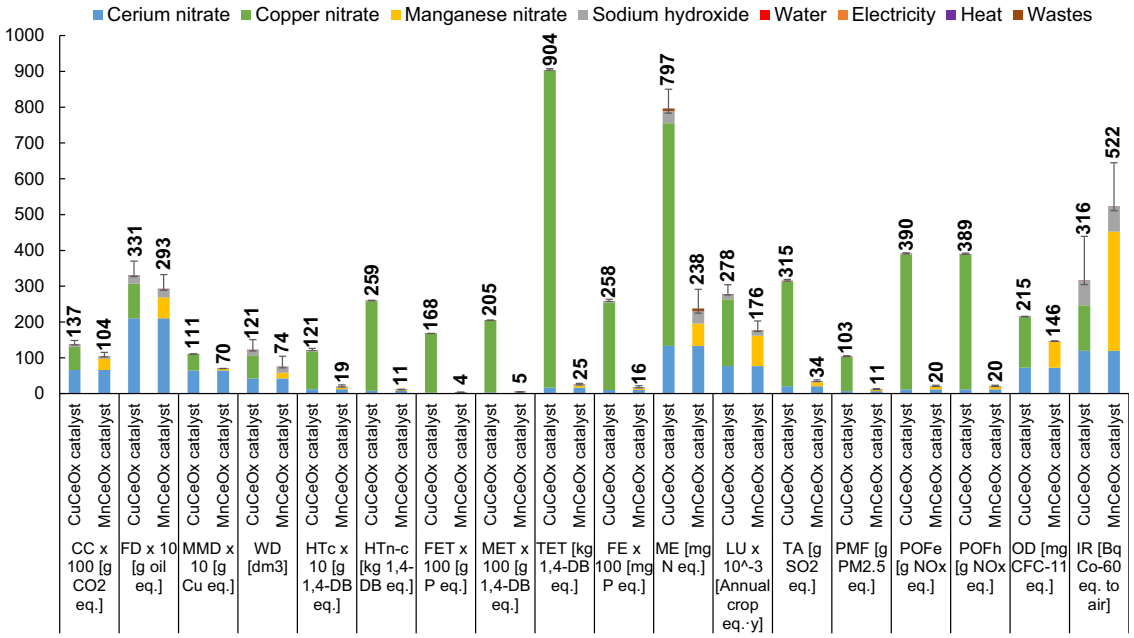

Fig. 7. Life cycle environmental impacts of $CuCeO_x$ and $MnCeO_x$ production. [All impacts are expressed per kg of catalyst produced. Some impacts have been scaled to fit. To obtain the original values, multiply with the factor on the x-axis, where relevant. Impacts: CC: climate change; FD: fossil depletion; MMD: metals and minerals depletion; WD: water depletion; HTc: human toxicity - cancer; HTn-c: human toxicity-non-cancer; FET: freshwater ecotoxicity; MET: marine ecotoxicity; TET: terrestrial ecotoxicity; FE: freshwater eutrophication; ME: marine eutrophication; LU: land use; TA: terrestrial acidification; PMF: particulate matter formation; POFe: photochemical oxidant formation - ecosystems; POFh: photochemical oxidant formation - human health; OD: ozone depletion; IR: ionizing radiation. DB: dichlorobenzene].

copper nitrate. Utilising the theoretical amount of NaOH (0.4 kg per kg catalyst) could reduce the impacts of catalyst preparation by ≤4 %, while the impacts would increase by 1–39 % if the excess of NaOH used in the laboratory experiments (1.3 kg per kg catalyst) is considered. The contributions of energy use, water and waste treatment is negligible (<1 %) across the categories considered (Fig. 7).

Given that the Mn-based catalyst is environmentally more sustainable than the Cu alternative, the rest of the LCA study related to CWO refers to the impacts using the $MnCeO_x$ option.

3.3.2. Fracking wastewater treatment

Table 9 summarises the environmental impacts of the CWO treatment methods in comparison to the ozonation processes. As can be seen, the impacts of the CWO are 1–3 orders of magnitude lower compared to those of ozonation for both coagulation and microfiltration in all the categories considered. This is due to the production of ozone which consumes significant amounts of electricity and oxygen (1.1 MWh and 561 kg m^{-3} treated wastewater, respectively), which contribute 18–77 % and 22–81 % to the impacts.

Comparing the two CWO-based processes, coagulation shows 1 % (climate change) to 65 % (ionizing radiation) lower impacts than microfiltration in 11 out of 18 categories. This is mainly due to the lower electricity consumption for coagulation (0.12 vs 0.63 kWh per m^{-3} treated wastewater). The remaining seven impacts are higher for coagulation from 1 % (terrestrial acidification) to 36 % (human toxicity - cancer) due to impacts from the use of the coagulant, which requires aluminium and sulphates for its production.

Table 9
Environmental impacts of CWO and ozonation per m^3 of treated wastewater.

Impact	Unit	CWO[a]		Ozonation	
		Coagulation	Microfiltration	Coagulation	Microfiltration
Climate change	kg CO_2 eq.	85.5	86.1	1334	1334
Fossil depletion	kg oil eq.	6.08	6.31	474	474
Metal and mineral depletion	g Cu eq.	30.8	23.2	965	957
Water depletion	dm^3	39.0	38.9	18,781	18,781
Human toxicity-cancer	g 1,4-DB eq.	178	131	53,979	53,932
Human toxicity-non-cancer	kg 1,4-DB eq.	1.74	2.40	1154	1155
Freshwater ecotoxicity	g 1,4-DB eq.	60.4	58.0	21,155	21,153
Marine ecotoxicity	g 1,4-DB eq.	74.9	71.5	26,217	26,213
Terrestrial ecotoxicity	kg 1,4-DB eq.	3.58	2.84	1018	1017
Freshwater eutrophication	g P eq.	0.53	1.02	810	810
Marine eutrophication	mg N eq.	92.1	133	58,068	58,108
Land use	Annual crop eq.·y	0.09	0.09	20.2	20.2
Terrestrial acidification	g SO_2 eq.	18.1	17.9	3557	3557
Particulate matter formation	g $PM_{2.5}$ eq.	6.63	7.89	3147	3148
Photochemical oxidant formation-ecosystems	g NO_x eq.	13.8	14.0	2133	2133
Photochemical oxidant formation-human health	g NO_x eq.	13.1	13.3	2109	2110
Ozone depletion	mg CFC-11 eq.	6.95	7.17	480	480
Ionizing radiation	kBq Co-60 eq. to air	0.10	0.27	213	213

[a] The results refer to the utilisation of $MnCeO_x$ catalyst.

The contribution analysis in Fig. 8 reveals that energy consumption in wastewater heating (CWO) and ozone production (ozonation) is the main contributor to most impacts (11–98 %) for all the treatment options. For CWO, CO_2 emissions from the oxidation of the organic fraction and solid wastes removed by coagulation or microfiltration are also significant contributors to climate change (~80 %) and land use (81 % and 69 %, respectively). The $MnCeO_x$ catalyst shows significant contribution to metal (23–30 %) and ozone depletion (20–21 %), but less so (1–9 %) for the other impacts. For the CWO process, the coagulant affects mainly metal depletion (19 %), human toxicity – cancer (44 %) and non-cancer (27 %), freshwater (25 %), marine (25 %) and terrestrial ecotoxicity (30 %), freshwater eutrophication (23 %) and ionizing radiation (24 %). Equipment utilised by CWO, (reported under "Facilities" in Fig. 8) has a negligible contribution (<1 %).

For ozonation, in addition to energy, oxygen consumption is the most significant contributor to the impacts (18–77 %). The equipment utilised for the production of ozone is also significant (12–22 %) for four impact categories (metal depletion, freshwater, marine and terrestrial ecotoxicity).

The lower energy consumption of CWO compared to ozonation (706 MJ_{th} vs 1.1 MWh per m^3 treated wastewater) would also improve the economics of the fracking wastewater treatment and, thus, of the fracking process overall. Based on the industrial costs of electricity of 0.0896 USD kWh^{-1} (EIA, 2022a) and natural gas of 0.0062 USD MJ_{th}^{-1} (EIA, 2022a, b), and considering the average flow rate of 46 L h^{-1}, CWO could potentially reduce the annual energy costs of fracking wastewater treatment by 38,000 USD per year compared to ozonation.

3.3.3. Sensitivity analysis

This section considers the influence on the CWO impacts of two parameters: energy consumption related to the downhole water temperature in fracking wells and catalyst lifetime.

3.3.3.1. Energy consumption. As mentioned earlier, significant differences in the downhole temperatures, which lead to different energy consumption in the CWO process, can be observed between wells according to their depth, pressure and location (EPA, 2016; Kahrilas et al., 2016). Thus, assumptions related to the fracking wastewater temperature present a degree of uncertainty, unless direct measurements on a specific well are available. Given that energy consumption is a significant environmental hotspot for CWO, as discussed in Section 3.3.2 and shown in Fig. 9, it is important to investigate the influence of the water temperature on the impacts. Therefore, this sensitivity analysis considers the effects of both lower (18 °C) and higher (200 °C) temperatures.

As can be inferred from Fig. 9, wastewater temperature has a significant effect on most environmental impacts, in some cases increasing or decreasing them by a factor of two for lower and higher temperatures, respectively. The impacts particularly affected include depletion of fossil and water resources, ecotoxicities, marine eutrophication, particulate matter formation and ozone depletion. This is to be expected as energy consumption is a significant environmental hotspot for these impacts (Fig. 9). By contrast, climate change and some other impacts, such as metal depletion and land use, are affected much less by the wastewater temperature as energy did not contribute significantly to their total values.

Therefore, these results suggest that CWO would lead to lower environmental impacts when applied to deep wells with higher downhole temperatures (Kahrilas et al., 2016). However, as discussed in Section 3.3.2, the impacts of CWO are expected to be lower than those of ozonation even for extremely low wastewater temperatures due to the avoided impacts of ozone production.

3.3.3.2. Catalyst lifetime. As mentioned in Section 2.3.2.2.2, the lifetime of catalyst considered in this study is currently unknown as they are in early development stages. As the catalyst contributes for 5–30 % to seven impacts (see Fig. 8), the assumption on their lifetime presents a degree of uncertainty. Therefore, this sensitivity analysis considers a shorter (0.5 years) and longer (five years) lifetime to determine the effect on the impacts compared to the base-case assumption of three years. As mentioned earlier, the results refer to the $MnCeO_x$ catalyst.

As shown in Fig. 10, increasing the catalyst lifetime from three to five years would decrease the depletion of metals by 9–12 % and ozone by 8

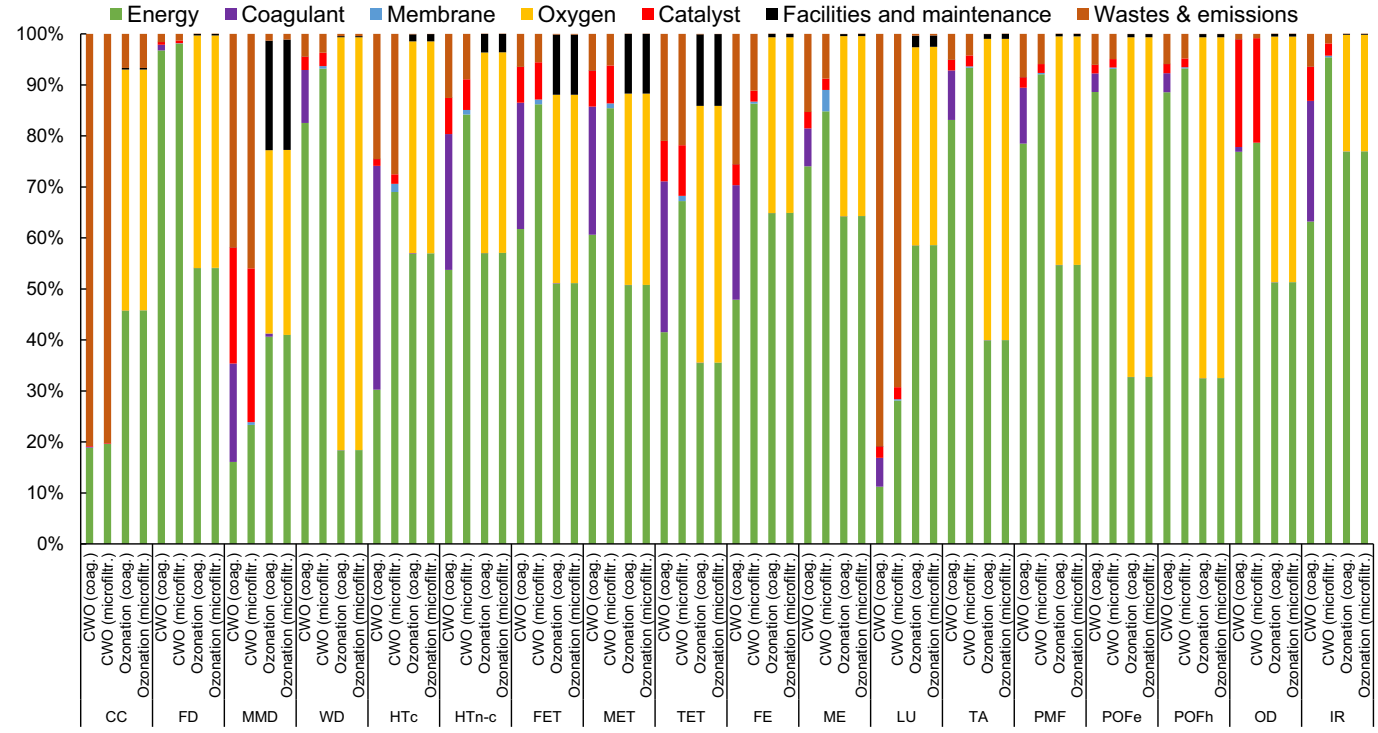

Fig. 8. Contribution analysis for the catalytic wet oxidation (CWO) and ozonation treatment methods. [All impacts are expressed per m^3 of wastewater treated. The catalyst is $MnCeO_x$. See Fig. 7 for the impact acronyms].

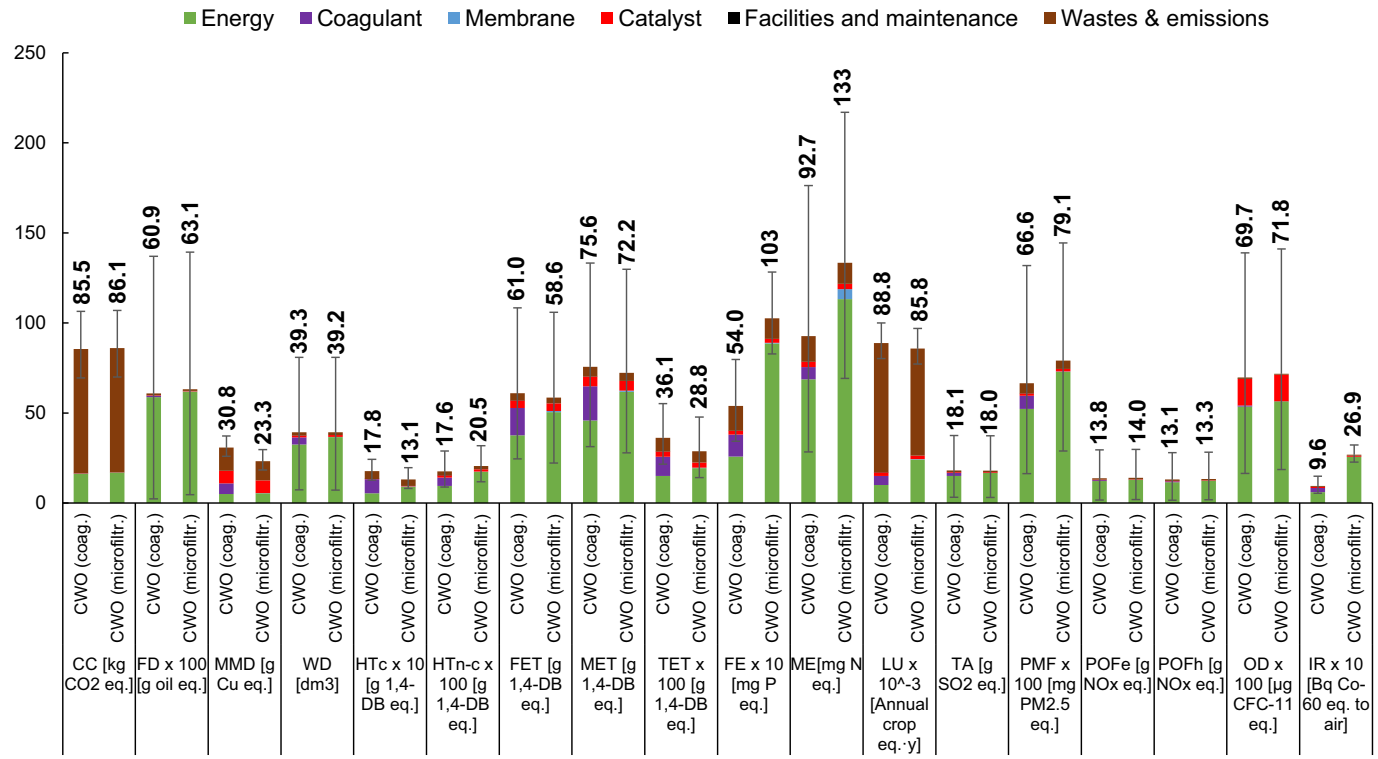

Fig. 9. The effect of wastewater temperatures (18–200 °C) on the life cycle environmental impacts of catalytic wet oxidation. [All impacts are expressed per m^3 of wastewater treated. The data labels represent the base case impacts (70 °C) and the error bars refer to temperature of 18 and 200 °C. See Fig. 7 for impact acronyms].

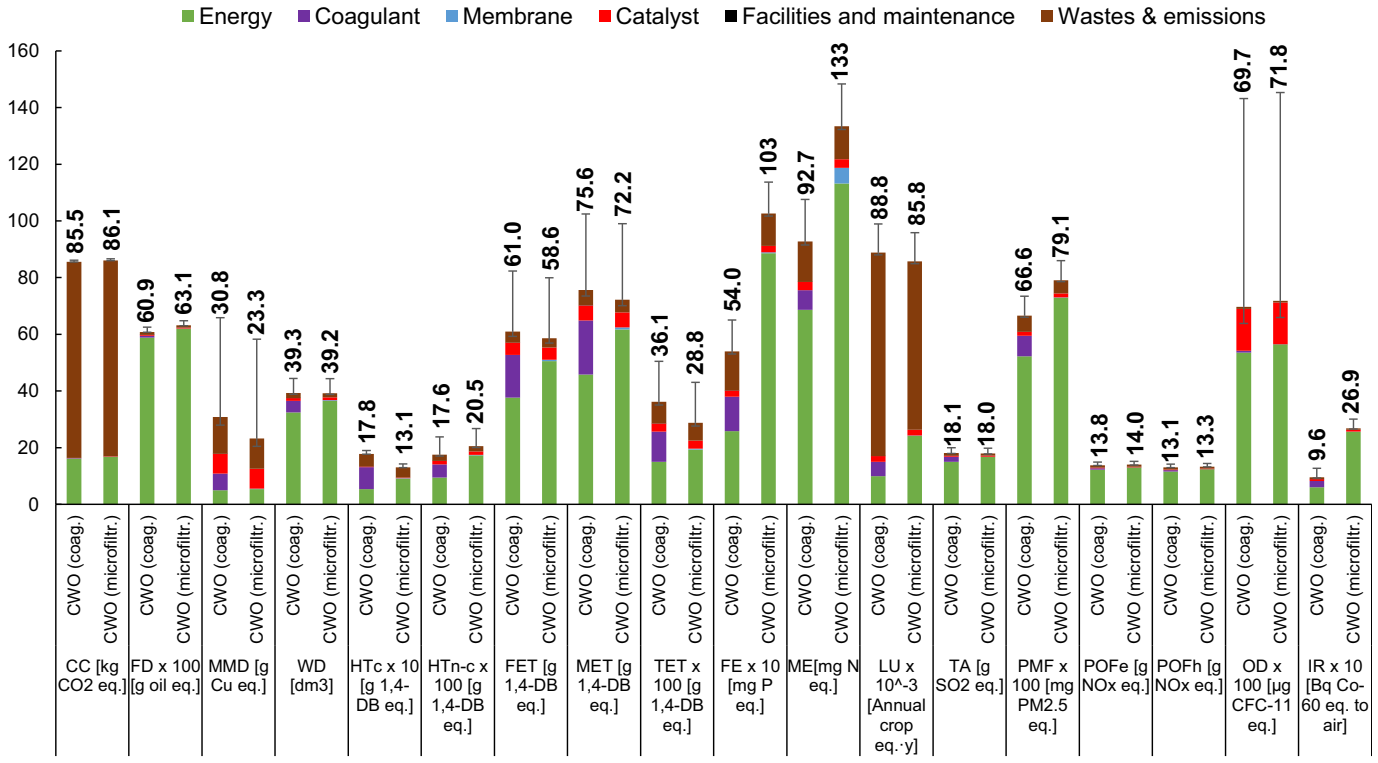

Fig. 10. The effect of catalyst lifetimes (0.5–5 years) on the life cycle environmental impacts of catalytic wet oxidation. [All impacts are expressed per m^3 of wastewater treated. The catalyst is $MnCeO_x$. The data labels represent the base case impacts. See Fig. 7 for acronyms].

% for both CWO processes, while a small (1–3 %) decrease would be observed in 13 categories. The effect on climate change, fossil depletion and human toxicity – cancer, would be negligible (≤1 %). On the other hand, the shorter lifetime would increase the impacts from 1 % (climate change) to 150 % (metal depletion) as the amount of catalyst would go up from 10 (three years) to 60 g m^{-3} treated wastewater.

Overall, these results suggest that research aimed at designing catalysts with longer lifetimes is necessary to increase the environmental sustainability of the CWO process. Moreover, reducing the amount of catalyst utilised would also aid decreasing the operating costs of the CWO process.

4. Conclusions

$MnCeO_x$ and $CuCeO_x$ catalysts were utilised as promising candidates for treating produced water from fracking operations and tested for phenol removal in the synthetic phenolic and fracking wastewaters, with the former NaCl-free and the latter containing 200 g L^{-1} NaCl. In general, the catalytic performance of $MnCeO_x$ significantly surpassed $CuCeO_x$ in terms of phenol (100 % vs. 69.1 %) and TOC (94 % vs. 63 %) removals in the fracking wastewater treatment. Moreover, insignificant metal leaching was observed when $MnCeO_x$ was utilised. By contrast, severe copper leaching (55 wt% after two cycles) was found due to the presence of high concentration of NaCl, demonstrating that $MnCeO_x$ was a better option than $CuCeO_x$ for CWO treatment of fracking wastewater.

The $MnCeO_x$ catalyst also had lower life cycle impacts (11–98 %) compared with the $CuCeO_x$ catalyst in 17 out of 18 impact categories considered. This is mainly due to the lower burdens related to the production and processing of manganese nitrate in comparison to copper nitrate used as precursors in the production of the catalysts.

The LCA comparison of CWO with ozonation showed that the former had 1–3 orders of magnitude lower impacts in all the categories due to the lower energy and materials requirements. Of the two wastewater pretreatment alternatives considered, coagulation was a better option for the removal of suspended solids from the wastewater, with up to 65 % lower impacts than microfiltration, mainly due to the energy required to push the water through the membrane and for backwashing.

Energy consumption is the main environmental hotspot for CWO mainly due to the heat utilised to bring the wastewater to the operating temperature. Therefore, applying CWO in wells with higher downhole temperatures would lead to significantly lower impacts. Nonetheless, even for extremely low wastewater temperatures (18 °C), CWO has nearly 60 % lower energy requirements than ozonation, which would result in 92–99 % lower impacts.

A sensitivity analysis showed that a shorter catalyst lifetime (0.5 years) can increase significantly (up to 150 %) the impacts of CWO. On the contrary, further increases to the catalyst lifetime from three to five years did not lead to significant improvements to the CWO impacts.

Overall, these results highlight the potential of CWO to treat fracking wastewater efficiently. They also suggest that CWO is an environmentally more sustainable option than ozonation. However, it is important to bear in mind that this work considered only phenol as a representative organic substance and the performance of catalysts in a complex matrix, such as fracking wastewater, may differ. Therefore, further work is needed in this respect. Moreover, future research should be directed towards improving the stability of the $MnCeO_x$ catalyst by optimising its key properties (e.g. optimise the metal load and increase the surface area of the catalyst), which would provide high activity and improved resistance to coking for the treatment of fracking wastewaters. Similarly, an LCA of the whole fracking wastewater treatment process (beyond the oxidation process) should be conducted and coupled with a cost benefit analysis in order to determine the most cost-effective and environmentally sustainable route for the treatment of this waste stream.

CRediT authorship contribution statement

Xiaoxia Ou: Investigation, Data curation, Formal analysis, Methodology, Visualization, Writing – original draft. **Marco Tomatis:** Investigation, Data curation, Formal analysis, Methodology, Visualization, Writing – original draft. **Billy Payne:** Data curation. **Helen Daly:** Data curation. **Sarayute Chansai:** Data curation. **Xiaolei Fan:** Supervision, Writing – review & editing. **Carmine D'Agostino:** Supervision, Writing – review & editing. **Adisa Azapagic:** Methodology, Supervision, Writing – review & editing. **Christopher Hardacre:** Funding acquisition, Supervision, Writing – review & editing.

Data availability

Open access experimental data can be found via the University of Manchester research portal. Further data will be made available upon reasonable request.

Declaration of competing interest

The authors declare that they have no known competing financial interests or personal relationships that could have appeared to influence the work reported in this paper.

Acknowledgments

UK Catalysis Hub is kindly thanked for resources and support provided via our membership of the UK Catalysis Hub Consortium and funded by EPSRC grants: EP/R026939/1, EP/R026815/1, EP/R026645/1 and EP/R027129/1.

Appendix A. Supplementary data

Supplementary data to this article can be found online at https://doi.org/10.1016/j.scitotenv.2022.160480.

References

EIA, 2022a. Electric Power Monthly with Data for July 2022. Washington, DC https://www.eia.gov/electricity/monthly/epm_table_grapher.php?t=epmt_5_6_a.
EIA, 2022b. Natural Gas Weekly Update. Washington, DC https://www.eia.gov/naturalgas/weekly/.
Adebayo, I.O., Olukowi, O.O., Zhiyuan, Z., Zhang, Y., 2021. Comparisons of coagulation efficiency of conventional aluminium sulfate and enhanced composite aluminium sulfate/polydimethyldiallylammonium chloride coagulants coupled with rapid sand filtration. J. Water Process Eng. 44, 102322.
Agarwal, M., Kudapa, V.K., 2022. Foam based fracking in unconventional shale reservoir. Mater. Today: Proc In press.
Aguilar-Alarcón, P., Zherebker, A., Rubekina, A., Shirshin, E., Simonsen, M.A., Kolarevic, J., et al., 2022. Impact of ozone treatment on dissolved organic matter in land-based recirculating aquaculture systems studied by fourier transform ion cyclotron resonance mass spectrometry. Sci. Total Environ. 843, 157009.
Al-Ghouti, M.A., Al-Kaabi, M.A., Ashfaq, M.Y., Da'na, D.A., 2019. Produced water characteristics, treatment and reuse: a review. J. Water Process Eng. 28, 222–239.
Alejandre, A., Medina, F., Fortuny, A., Salagre, P., Sueiras, J., 1998. Characterisation of copper catalysts and activity for the oxidation of phenol aqueous solutions. Appl. Catal. B Environ. 16, 53–67.
Arena, F., Giovenco, R., Torre, T., Venuto, A., Parmaliana, A., 2003. Activity and resistance to leaching of cu-based catalysts in the wet oxidation of phenol. Appl. Catal. B Environ. 45, 51–62.
Arena, F., Italiano, C., Spadaro, L., 2012. Efficiency and reactivity pattern of ceria-based noble metal and transition metal-oxide catalysts in the wet air oxidation of phenol. Appl. Catal. B Environ. 115, 336–345.
Argyle, M., Bartholomew, C., 2015. Heterogeneous catalyst deactivation and regeneration: a review. Catalysts 5, 145–269.
Bah, M., 2013. Magnetic and Structural Studies of Core/shell Manganese Oxide Nanoparticles Fabricated by Inert Gas Condensation. University of Delaware.
Barlak, M.S., Değermenci, N., Cengiz, İ., Ucun Özel, H., Yildiz, E., 2020. Comparison of phenol removal with ozonation in jet loop reactor and bubble column. J. Environ Chem. Eng. 8.
Barrios, R., Siebel, M., Van der Helm, A., Bosklopper, K., Gijzen, H., 2008. Environmental and financial life cycle impact assessment of drinking water production at waternet. J. Clean. Prod. 16, 471–476.
Basu, O.D., 2015. Backwashing. In: Drioli, E., Giorno, L. (Eds.), Encyclopedia of Membranes. Springer Berlin Heidelberg, Berlin, Heidelberg, pp. 1–3.
Bellani, J., Verma, H.K., Khatri, D., Makwana, D., Shah, M., 2021. Shale gas: a step toward sustainable energy future. J. Pet. Explor. Prod. Technol. 11, 2127–2141.
Bhargava, S.K., Tardio, J., Prasad, J., Föger, K., Akolekar, D.B., Grocott, S.C., 2006. Wet oxidation and catalytic wet oxidation. Ind. Eng. Chem. Res. 45, 1221–1258.

Birdsell, D.T., Rajaram, H., Lackey, G., 2015. Imbibition of hydraulic fracturing fluids into partially saturated shale. Water Resour. Res. 51, 6787–6796.

Botondi, R., Barone, M., Grasso, C., 2021. A review into the effectiveness of ozone technology for improving the safety and preserving the quality of fresh-cut fruits and vegetables. Foods 10, 748.

Carneiro, M.F.C., Leão, V.A., 2007. The role of sodium chloride on surface properties of chalcopyrite leached with ferric sulphate. Hydrometallurgy 87, 73–82.

Chen, H., Sayari, A., Adnot, A., Fç, Larachi, 2001. Composition–activity effects of Mn–Ce–O composites on phenol catalytic wet oxidation. Appl. Catal. B Environ. 32, 195–204.

Chorghe, D., Sari, M.A., Chellam, S., 2017. Boron removal from hydraulic fracturing wastewater by aluminum and iron coagulation: mechanisms and limitations. Water Res. 126, 481–487.

Cuellar-Franca, R.M., Garcia-Gutierrez, P., Taylor, S.F., Hardacre, C., Azapagic, A., 2016. A novel methodology for assessing the environmental sustainability of ionic liquids used for CO2 capture. Faraday Discuss. 192, 283–301.

de Lima, S.L., Pereira, F.S., de Lima, R.B., de Freitas, I.C., Spadotto, J., Connolly, B.J., et al., 2022. MnO2-ir nanowires: combining ultrasmall nanoparticle sizes, O-vacancies, and low Noble-metal loading with improved activities towards the oxygen reduction reaction. Nanomaterials 12, 3039.

Dubber, D., Gray, N.F., 2010. Replacement of chemical oxygen demand (COD) with total organic carbon (TOC) for monitoring wastewater treatment performance to minimize disposal of toxic analytical waste. J. Environ. Sci. Health A Tox. Hazard. Subst. Environ. Eng. 45, 1595–1600.

Ellafi, A., Jabbari, H., Tomomewo, O.S., Mann, M.D., Geri, M.B., Tang, C., 2020. Future of hydraulic fracturing application in terms of water management and environmental issues: a critical review. SPE Canada unconventional resources conference. OnePetro.

EPA, 2016. Hydraulic Fracturing for Oil and Gas: Impacts from the Hydraulic Fracturing Water Cycle on Drinking Water Resources in the United States. Office of Research and Development, Washington, DC.

Esteves, B.M., Morales-Torres, S., Maldonado-Hódar, F.J., Madeira, L.M., 2022. Sustainable iron-olive stone-based catalysts for Fenton-like olive mill wastewater treatment: development and performance assessment in continuous fixed-bed reactor operation. Chem. Eng. J. 435, 134809.

Gould, J.P., Weber, W.J., 1976. Oxidation of phenols by ozone. J. Water Pollut. Control Fed. 48, 47–60.

Guo, C., Chang, H., Liu, B., He, Q., Xiong, B., Kumar, M., et al., 2018. A combined ultrafiltration–reverse osmosis process for external reuse of Weiyuan shale gas flowback and produced water. Environ. Sci.: Water Res. Technol. 4, 942–955.

Hakami, M.W., Alkhudhiri, A., Al-Batty, S., Zacharof, M.P., Maddy, J., Hilal, N., 2020. Ceramic microfiltration membranes in wastewater treatment: filtration behavior, fouling and prevention. Membranes (Basel) 10.

Hammouda, S.B., Zhao, F., Safaei, Z., Babu, I., Ramasamy, D.L., Sillanpää, M., 2017. Reactivity of novel ceria-perovskite composites CeO2-LaMO3 (MCu, Fe) in the catalytic wet peroxidative oxidation of the new emergent pollutant 'Bisphenol F': characterization, kinetic and mechanism studies. Appl. Catal. B Environ. 218, 119–136.

He, C., Vidic, R.D., 2016. Application of microfiltration for the treatment of Marcellus shale flowback water: influence of floc breakage on membrane fouling. J. Membr. Sci. 510, 348–354.

Hočevar, S., Batista, J., Levec, J., 1999. Wet oxidation of phenol on Ce1− xCuxO2− δCatalyst. J. Catal. 184, 39–48.

Hočevar, S., Krašovec, U.O., Orel, B., Aricó, A.S., Kim, H., 2000. CWO of phenol on two differently prepared CuO–CeO2 catalysts. Appl. Catal. B Environ. 28, 113–125.

Hou, X., Zhao, Q., Liu, Z., Cheng, D.-g., Chen, F., Zhan, X., 2022. Modulating cu species in copper–ceria catalyst for boosting CO preferential oxidation: elucidating the role of ceria crystal plane. Int. J. Hydrog. Energy In press.

Huijbregts, M.A.J., Steinmann, Z.J.N., Elshout, P.M.F., Stam, G., Vieira, M.D.M., Hollander, A., 2016. ReCiPe 2016 - A Harmonized Life Cycle Impact Assessment Method at Midpoint and Endpoint Level - Report I: Characterization. Ministry of Health, Wlefare and Sport, Bilthoven, The Netherlands.

Hussain, K., Khan, N.A., Vambol, V., Vambol, S., Yeremenko, S., Sydorenko, V., 2022. Advancement in ozone base wastewater treatment technologies: brief review. Ecol. Quest. 33, 1–23.

Ikehata, K., Li, Y., 2018. Ozone-based processes. Advanced Oxidation Processes for Waste Water Treatment. Elsevier, pp. 115–134.

Imamura, S., Doi, A., Ishida, S., 1985. Wet oxidation of ammonia catalyzed by cerium-based composite oxides. Ind. Eng. Chem. Prod. Res. Dev. 24, 75-80.

Imamura, S., Nakamura, M., Kawabata, N., Yoshida, J., Ishida, S., 1986. Wet oxidation of poly (ethylene glycol) catalyzed by manganese-cerium composite oxide. Ind. Eng. Chem. Prod. Res. Dev. 25, 34–37.

Imran, B., Khan, S.J., Qazi, I.A., Arshad, M., 2015. Removal and recovery of sodium hydroxide (NaOH) from industrial wastewater by two-stage diffusion dialysis (DD) and electrodialysis (ED) processes. Desalin. Water Treat. 57, 7926–7932.

INTEK, 2011. Review of Emerging Resources: U.S. Shale Gas and Shale Oil Plays. U.S. Energy Information Administration.

ISO, 2006a. Environmental Management – Life Cycle Assessment – Principles and Framework. 14040, Geneva.

ISO, 2006b. Environmental Management – Life Cycle Assessment – Requirements and Guidelines. 14044, Geneva.

Jin, X., Zhang, W., Ji, Z., Zhou, L., Jin, P., Wang, X.C., et al., 2018. Application and mechanism of nucleation-induced pelleting coagulation (NPC) in treatment of fracturing wastewater with high concentration of dissolved organic matter. Chemosphere 211, 1082–1090.

Joshi, M.G., Shambaugh, R.L., 1982. The kinetics of ozone-phenol reaction in aqueous solutions. Water Res. 16, 933–938.

Kahrilas, G.A., Blotevogel, J., Corrin, E.R., Borch, T., 2016. Downhole transformation of the hydraulic fracturing fluid biocide glutaraldehyde: implications for flowback and produced water quality. Environ. Sci. Technol. 50, 11414–11423.

Kaldas, K., Preegel, G., Muldma, K., Lopp, M., 2020. Wet air oxidation of oil shales: kerogen dissolution and dicarboxylic acid formation. ACS Omega 5, 22021–22030.

Kim, K.H., Ihm, S.K., 2011. Heterogeneous catalytic wet air oxidation of refractory organic pollutants in industrial wastewaters: a review. J. Hazard. Mater. 186, 16–34.

King, H., 2008. Marcellus Shale - Appalachian Basin Natural Gas Play. Geology.com, p. 2102.

Kurian, M., 2020. Cerium oxide based materials for water treatment – a review. J. Environ. Chem. Eng. 8.

Lamonier, C., Bennani, A., D'Huysser, A., Aboukaïs, A., Wrobel, G., 1996. Evidence for different copper species in precursors of copper–cerium oxide catalysts for hydrogenation reactions. An X-ray diffraction, EPR and X-ray photoelectron spectroscopy study. J. Chem. Soc. Faraday Trans. 92, 131–136.

Lapointe, M., Papineau, I., Peldszus, S., Peleato, N., Barbeau, B., 2021. Identifying the best coagulant for simultaneous water treatment objectives: interactions of mononuclear and polynuclear aluminum species with different natural organic matter fractions. J. Water Process Eng. 40, 101829.

Lee, K., Neff, J., 2011. Produced Water.

Li, L., Wu, F., Cao, Y., Cheng, F., Wang, D., Li, H., 2022. Sustainable development index of shale gas exploitation in China, the UK, and the US. Environ. Sci. Ecotechnology 12, 100202.

Lim, S., Shi, J.L., von Gunten, U., McCurry, D.L., 2022. Ozonation of organic compounds in water and wastewater: a critical review. Water Res. 213, 118053.

Lin, F., Wang, Z., Zhang, Z., He, Y., Zhu, Y., Shao, J., et al., 2020. Flue gas treatment with ozone oxidation: an overview on NOx, organic pollutants, and mercury. Chem. Eng. J. 382, 123030.

Liu, Y., Wu, D., Chen, M., Ma, L., Wang, H., Wang, S., 2017. Wet air oxidation of fracturing flowback fluids over promoted bimetallic cu-cr catalyst. Catal. Commun. 90, 60–64.

Matatov-Meytal, Y.I., Sheintuch, M., 1998. Catalytic abatement of water pollutants. Ind. Eng. Chem. Res. 37, 309–326.

Munoz, I., Rodriguez, A., Rosal, R., Fernandez-Alba, A.R., 2009. Life cycle assessment of urban wastewater reuse with ozonation as tertiary treatment: a focus on toxicity-related impacts. Sci. Total Environ. 407, 1245–1256.

Nijdam, D., Blom, J., Boere, J., 1999. Environmental Life Cycle Assessment (LCA) of two advanced wastewater treatment techniques. Stud. Surf. Sci. Catal. 120, 763–775 Elsevier.

Ou, X., Daly, H., Fan, X., Beaumont, S., Chansai, S., Garforth, A., et al., 2022. High-ionic-strength wastewater treatment via catalytic wet oxidation over a MnCeO x catalyst. ACS Catal. 12, 7598–7608.

Papadopoulos, C., Kappis, K., Papavasiliou, J., Vakros, J., Antonelou, A., Gac, W., et al., 2022. Impact of hydrothermally prepared support on the catalytic properties of CuCe oxide for preferential CO oxidation reaction. Catalysts 12, 674.

Papavasiliou, A., Van Everbroeck, T., Blonda, C., Oliani, B., Sakellis, E., Cool, P., et al., 2022. Mesoporous CuO/TiO2 catalysts prepared by the ammonia driven deposition precipitation method for CO preferential oxidation: effect of metal loading. Fuel 311, 122491.

Parameshwaran, K., Fane, A.G., Cho, B.D., Kim, K.J., 2001. Analysis of microfiltration performance with constant flux processing of secondary effluent. Water Res. 35, 4349–4358.

Phung Hai, T.A., Samoylov, A.A., Rajput, B.S., Burkart, M.D., 2022. Laboratory ozonolysis using an integrated Batch–DIY flow system for renewable material production. ACS Omega 7, 15350–15358.

Piccinno, F., Hischier, R., Seeger, S., Som, C., 2016. From laboratory to industrial scale: a scale-up framework for chemical processes in life cycle assessment studies. J. Clean. Prod. 135, 1085–1097.

Pintar, A., Batista, J., Hočevar, S., 2005. TPR, TPO, and TPD examinations of Cu0. 15Ce0. 85O2− y mixed oxides prepared by co-precipitation, by the sol–gel peroxide route, and by citric acid-assisted synthesis. J. Colloid Interface Sci. 285, 218–231.

Pitts, F., 1979. Preparation of Rare Earth Nitrates. US4231997A. BASF Catalysts LLC, US.

Senanayake, G., 2007. Chloride assisted leaching of chalcocite by oxygenated sulphuric acid via cu (II)–OH–Cl. Miner. Eng. 20, 1075–1088.

Serajuddin, M., Chowdhury, M.A., Haque, M.M., Haque, M.E., 2019. Using turbidity to determine total suspended solids in an urban stream: a case study. Proceedings of the 2nd International Conference on Water and Environmental Engineering, Dhaka, pp. 19–22.

Silva, A.M., Marques, R.R., Quinta-Ferreira, R.M., 2004. Catalysts based in cerium oxide for wet oxidation of acrylic acid in the prevention of environmental risks. Appl. Catal. B Environ. 47, 269–279.

Sun, Y., Wang, D., Tsang, D.C.W., Wang, L., Ok, Y.S., Feng, Y., 2019. A critical review of risks, characteristics, and treatment strategies for potentially toxic elements in wastewater from shale gas extraction. Environ. Int. 125, 452–469.

Tadjarodi, A., Roshani, R., 2014. A green synthesis of copper oxide nanoparticles by mechanochemical method. Curr. Chem. Lett. 3, 215–220.

Takić, L., Vasović, D., Marković, S., Burzić, Z., 2019. The equation for the optimum dosage of coagulant for water treatment plant. Tehnički Vjesn. 26, 571–575.

Tang, X., Li, Y., Huang, X., Xu, Y., Zhu, H., Wang, J., et al., 2006. MnOx–CeO2 mixed oxide catalysts for complete oxidation of formaldehyde: effect of preparation method and calcination temperature. Appl. Catal. B Environ. 62, 265–273.

Tangsubkul, N., Parameshwaran, K., Lundie, S., Fane, A.G., Waite, T.D., 2006. Environmental life cycle assessment of the microfiltration process. J. Membr. Sci. 284, 214–226.

Thinkstep, 2019. GaBi.

Tsiotsias, A.I., Charisiou, N.D., AlKhoori, A., Gaber, S., Stolojan, V., Sebastian, V., et al., 2022. Optimizing the oxide support composition in pr-doped CeO2 towards highly active and selective Ni-based CO2 methanation catalysts. J. Energy Chem. 71, 547–561.

Vadasarukkai, Y.S., Gagnon, G.A., 2017. Influence of the mixing energy consumption affecting coagulation and floc aggregation. Environ. Sci. Technol. 51, 3480–3489.

Wang, Q., Li, S., 2019. Shale gas industry sustainability assessment based on WSR methodology and fuzzy matter-element extension model: the case study of China. J. Clean. Prod. 226, 336–348.

Warner, N.R., Christie, C.A., Jackson, R.B., Vengosh, A., 2013. Impacts of shale gas wastewater disposal on water quality in western Pennsylvania. Environ. Sci. Technol. 47, 11849–11857.

Wernet, G., Bauer, C., Steubing, B., Reinhard, J., Moreno-Ruiz, E., Weidema, B., 2016. The ecoinvent database version 3 (part I): overview and methodology. Int. J. Life Cycle Assess. 21, 1218–1230.

Xiong, W., Cui, W., Li, R., Feng, C., Liu, Y., Ma, N., et al., 2020. Mineralization of phenol by ozone combined with activated carbon: performance and mechanism under different pH levels. Environ. Sci. Ecotechnology 1.

Zhou, L., Zhang, S., Li, Z., Liang, X., Zhang, Z., Liu, R., et al., 2020. Efficient degradation of phenol in aqueous solution by catalytic ozonation over MgO/AC. J. Water Process Eng. 36.